Helena Canadell Cuadrado

Effect of the adsorption and desorption of water on the thermal inertia of buildings

Final Master Project

Adviser: Dr. Dieter Boer

Co-adviser: Alba Torres

Master's Degree in Industrial Engineering

UNIVERSITAT ROVIRA I VIRGILI

Tarragona

2017

Index

1 Introduction

Energy saving and efficiency is gathering importance for environmental and economic reasons as the availability of natural resources is decreasing and the cost of energy increases in long term. Despite the increased energy cost, the consumption in the residential sector had an increasing tendency until recent years when it has maintained a certain level, as shown in figure 1.

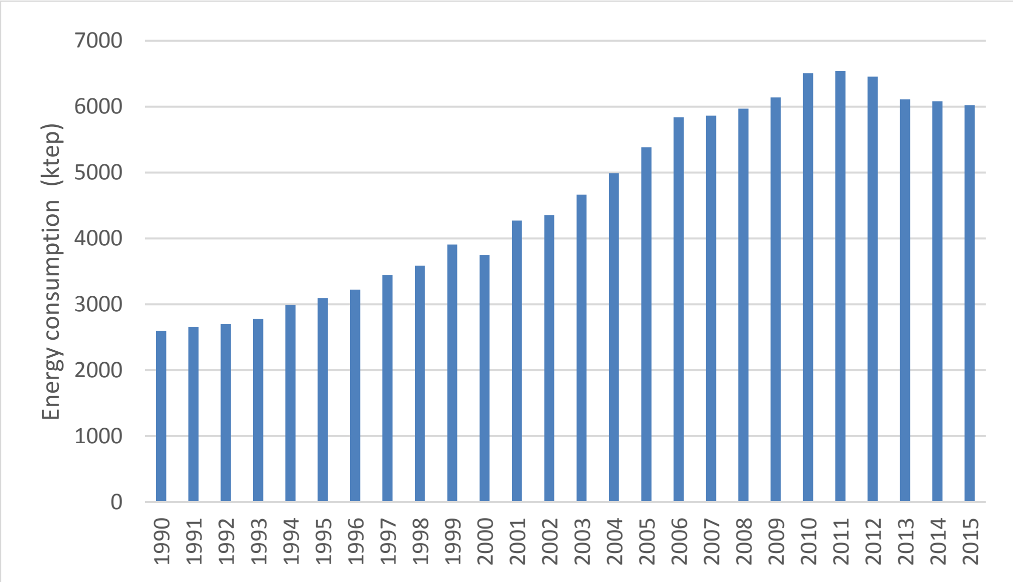

Figure 1. Energy consumption of the residential sector in Spain [1].

In 2009, the European Union Council approved the legislative measure package about energy and climate change. The objective is to reduce emissions of the European Union by 20% for the year 2020. For the year 2020, the EU has also proposed to obtain 20% of the energy from renewable sources. Through the improvement of energy efficiency, the energy consumption shall be reduced up to a 20% below the predicted levels [2]. Energy consumption in residential buildings in 2014 represented the 18.7% of the final energy consumption in Spain [3]. This is why in the building sector measures have to be implemented to obtain a higher energy efficiency and try to achieve a significantly lower consumption while maintaining the comfort conditions and without decreasing the quality of life.

As can be observed in figure 2, the higher percentage of residential energy consumption (44%) goes to heating and cooling, being the heating consumption the biggest part of it by far (43%). Home appliances follow with a 26.6% and domestic hot water with a 17.9%. So, the most effective way to reduce residential energy consumption would be to reduce the heating and cooling consumption.

Some of the approaches that can be taken to reduce heating and cooling consumption are [4]:

- Improving the thermal envelope, reducing the heat flux towards the interior in summer while the heat loss towards the exterior is avoided in winter. This can be achieved with measures like improving the thermal insulation, substitution of carpentry and glazing, and adequate insulation of zones with thermal bridges.

- Improving heating, cooling, hot sanitary water and lightning equipment efficiency, which means a substitution of the existent equipment for new one with a higher efficiency.
- Designing buildings considering bioclimatic architecture, like selecting a building's location and orientation adequate to the local climate, a window's design adequate to the orientation, and the use of construction elements with high thermal inertia.

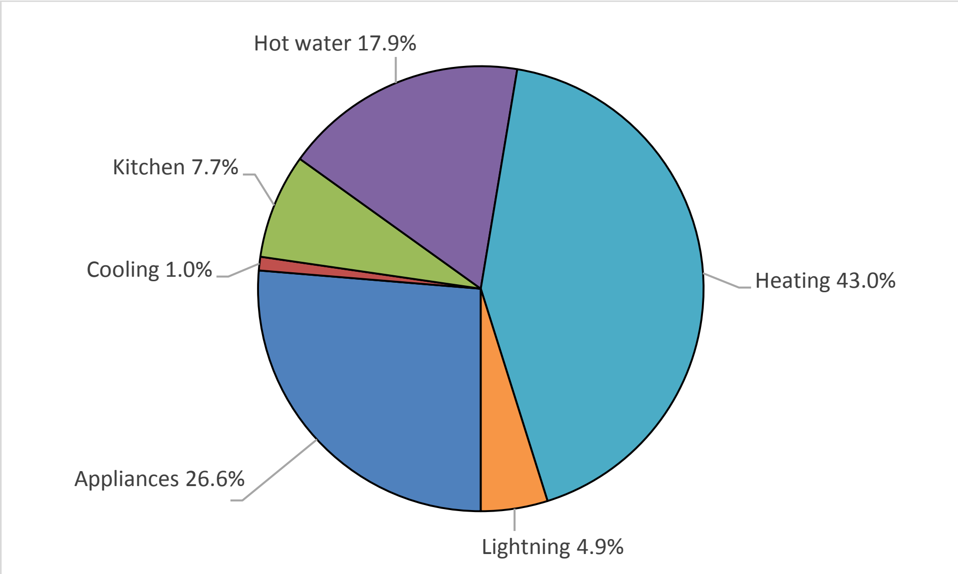

Figure 2. Energy consumption according to its use in the residential sector in Spain (2014) [3].

From all the options to reduce energy consumption, this study has focused on the improvement of the thermal inertia of the building by modifying the thermal envelope. In this case, it will be done by changing materials from the external walls of the building under study, which is a representative example of the Spanish building stock. Construction elements, like walls, with high thermal inertia allow to maintain a stable temperature inside a building during all day. This is done by the absorption of heat from the interior environment, which is progressively stored inside the wall during the day, due to the temperature difference between them. Afterwards, it is dissipated during the night, reducing the need for heating and cooling mechanisms.

Going back to the EU objectives for 2020, same as energy efficiency has to be increased, environmental impact from construction should be reduced. This can be done by using low embodied energy materials, amongst other ways. Low embodied energy materials use less energy and fewer resources to be made, transported and built, thus lowering the environmental impact. Reddy et al. [5] presented the difficulty to sustain the building activity using the currently available energy-intensive materials and building techniques and technologies, especially when meeting the future demand. A low embodied energy material has been chosen for this study with the aim of reducing the environmental impact. Table 1 shows the embodied energy in various construction systems.

Table 1. Embodied energy in various walling and floor/roofing systems [5].

Type of building element	Energy per unit (GJ)
Burnt clay brick masonry (m^3)	2.00-3.40
Reinforced concrete slab (m^2)	0.80-0.85
Unreinforced masonry vault roof (m^2)	0.45-0.60
Composite SMB masonry jack-arch (m^2)	0.45-0.55
SMB filler slab (m^2)	0.60-0.70
SMB masonry (m^3)	0.50-0.60
Fly ash block masonry (m^3)	1.00-1.35
Stabilized rammed earth wall (m^3)	0.45-0.60
Unstabilized rammed earth wall (m^3)	0.00-0.18

As can be observed in the previous table, there is an important difference in the embodied energy between conventional materials and low embodied ones. Rammed earth constructions requires less energy for the fabrication and processing compared with other conventional materials. This reduction is even higher for the unstabilized rammed earth.

Even though earth construction has a major expression in less developed countries, earth is becoming attractive again in developed countries, especially combined with modern techniques. This happens due to the increasing awareness of environmental issues in the building industry. Modern engineering is being applied to structural design, thermal modelling, mix design, construction methodology and other aspects of earth construction [6].

Earth construction has been chosen for this study because of its low environmental impact and its potential to improve the thermal behavior of buildings due to its high thermal inertia, as presented by Cagnon et al. [7] in their study of earth bricks. The study of their hygrothermal properties also confirmed their capacity to regulate the relative humidity of indoor air.

In this project, the hygrothermal behavior of a simulated building is studied to assess the substitution of part of the external walls for an earth layer. The objective is to analyze the effect of the thermal inertia of the walls, and if energy consumption is reduced while comfort conditions are maintained.

Even though the comfort conditions according to UNE-EN ISO 7730 [8] establish a relative humidity of 50%, research performed by Grandjean (1972) [9] and Becker (1986) [10] show that a relative humidity of less than 40% over a long period may dry out the mucous membrane. This can decrease resistance to colds and related diseases. It also shows that a high relative humidity of up to 70% has positive consequences. It reduces the fine dust content of the air, activates the protection mechanisms of the skin against microbes and reduces the life of many bacteria and viruses, and reduces odor and static charge on the surfaces of objects in the room. On the contrary, a relative humidity of more than 70% is normally experienced as unpleasant. Increasing rheumatic pains are observed in cold humid air. And fungus formation increases significantly in closed rooms when the humidity rises above 70% or 80%. This is the relative humidity range that is looked for in this project.

To quantify the environmental impact of the rehabilitation, the study includes an environmental evaluation with a Life Cycle Assessment, which includes the energy and materials impacts during the life span of the building. This will quantify the difference between the performance of materials already present in the building and the one from rehabilitation with earth.

Life Cycle Assessment (LCA) is an objective process which evaluates the environmental loads associated to a product, process or activity by identifying and quantifying the use of mass and energy and the discharges to the environment. LCA accounts for all energy inputs and outputs of a building during its entire life cycle, including manufacturing, transport, use, and demolition phases [11].

The chosen model for the case study is a building representative for a detached single-family housing from 1960 to 1979 in Spain. It has been chosen for being one of the most common house type, as shown in figure 3. This housing type presents a larger opportunity for improvement than the ones built after 1980, given that houses built after this year respond to a consolidated technical regulatory frame inside of which thermal insulation is considered as a prescription. More details of the model are explained in section 4.2.

Año de construcción	Unifamiliares		Plurifamiliares		Sin datos	TOTAL	Nº de viviendas en el edificio
	1 - 3	≥ 4	1 - 3	≥ 4			Nº de plantas sobre rasante
< 1940	680.683	3.687	272.852	489.329			A - G
1941 - 1960	624.646	1.457	346.055	889.611			B - H
1961 - 1980	1.156.215	2.388	781.206	4.483.759			C - E - I
1981 - 2007	2.236.882	7.774	1.312.285	3.444.532			D - F - J
2008 - 2011	233.647	660	122.404	438.446			
Sin datos			130.073		425.073		
TOTAL						18.083.664	Clústers 16.099.148 (89%)

Figure 3. Number of households (main homes) according to year of construction, number of households and number of floors (elaborated with the census of 2011) [12].

2 State of the art

For decades, energy saving has been an important objective in buildings and a great deal of research has been directed towards it from different approaches, usually with the use of building simulations. Some of the approaches have relate the shape of buildings and the energy consumption [13] while others optimize the building envelope [14-15].

To improve the environmental impact of constructions as well as the energy consumption, research has also been aimed at the study of more sustainable materials, like earth. The hygrothermal properties of earth make it interesting in terms of potential improvement of the thermal comfort.

Hall et al. [16] characterized the hygrothermal properties of stabilized rammed earth by experimental testing and in [17] presented an analysis of the hygrothermal behaviors of stabilized rammed earth walls used in a building in the UK. It was determined that the SRE walls significantly reduced the amplitude of relative humidity fluctuations during both the summer and winter when compared to walls covered with materials that increased surface diffusion resistance.

On the other hand, Arrigoni et al. [18] has recently determined that stabilization has a detriment on the moisture buffer capacity of rammed earth. Which is likely to be caused by the inhibition of the physic-chemical interactivity between moisture and clays.

Along with the research of the hygrothermal properties of earth construction, models like the one that has been presented by Soudani et al. [19] In this research, there was proposed a coupled model based on heat and mass balances inside the earthen walls taking into consideration the effects due to phase change of water inside of them.

Some simulation tools have been adapted or developed to be able to predict combined heat, air and moisture transfer in buildings. Among them, EnergyPlus, with the HAMT model, and WufiPlus, which is a whole-building extension of the Wufi software, stand out in the developement of models to simulate hygrothermal transfers in building envelopes [20].

When aiming for sustainable construction materials, the environmental impact has to be considered as a decision-making factor while taking other parameters into consideration as well.

Some studies have focused on the integration of the environmental impact with other parameters. Carreras el at. [21] presented a methodology for determining the optimal insulation thickness for external building surfaces based on a multi-objective optimization model that minimizes simultaneously cost and environmental impact associated to energy consumption and the generation of the construction materials.

Chantrelle et al. [22] as well, developed a multicriteria tool for optimizing the renovation of buildings and applied it in a case study to optimize the renovation of the envelope of a building. The optimization was based on four optimization criteria: energy consumption, thermal comfort, cost, and life-cycle environmental impact.

3 Methodology

3.1 Building modelling

To elaborate this project, different computer programs have been necessary to simulate the chosen model and its thermal behavior.

The 3D model of the house has been created with Sketchup [23], which is a 3D modelling program. With this program, the geometry and base structure of the house has been created: walls, ground and roof, windows and thermal bridges.

Once the model is created, it is necessary to define the materials, constructions and the internal gains. The materials and constructions used are detailed in section 4.3. In this case, the internal gains are the ones caused by lightning, electric equipment and people. The values for the internal gains as well as the optimal conditions for comfort (temperature and air infiltrations) have been extracted from the Energy Saving Basic Document [24], and are shown in section 4.5 and 4.6 respectively. All these parameters have been defined in OpenStudio [25], which is a specialized software in the energy simulation of buildings.

From OpenStudio, the model file has been exported to EnergyPlus [26], which is a building centered calculation engine. It contains internal equations to calculate the different heat transfer mechanisms (conduction, convection and radiation). Even though OpenStudio also calculates heat transfer in buildings, it does not have the means to calculate moisture transfer, which is fundamental to see the effect of the hygroscopic properties in the thermal inertia of the building. EnergyPlus contains the Combined Heat and Moisture Transfer (HAMT) model, which as the name indicates, is a solution algorithm that calculates both heat and moisture transfer. It also provides the temperature and moisture profiles through surfaces.

The equations used in the HAMT model, are derived from heat and moisture balance equations and are taken from [27]. They describe a theoretical model for the transfer of heat and moisture through a material. The three terms in equation (1), describe the storage, transport and generation of heat respectively [28].

$$\frac{\partial H}{\partial T}\frac{\partial T}{\partial \tau} = \frac{\partial}{\partial x}\left(k^{\omega}\frac{\partial T}{\partial x}\right) + h_v \frac{\partial}{\partial x}\left(\frac{\delta}{\mu}\frac{\partial T}{\partial x}\right) \tag{1}$$

The three terms in equation (2), describe the storage of moisture, the transport of liquid moisture and the transport of vapor respectively [28].

$$\frac{\partial \omega}{\partial \varphi}\frac{\partial \varphi}{\partial \tau} = \frac{\partial}{\partial x}\left(D^{\omega}\frac{\partial \omega}{\partial \varphi}\frac{\partial \varphi}{\partial x}\right) + \frac{\partial}{\partial x}\left(\frac{\delta}{\mu}\frac{\partial T}{\partial x}\right) \tag{2}$$

Where:

x is the distance between cell centers in m,

k^{ω} is the moisture dependent thermal conductivity in W/m°C,

h_v is the evaporation enthalpy of water (=2489 kJ/kg),

δ is the vapor diffusion coefficient in air in kg/msPa,

μ is the moisture dependent vapor diffusion coefficient (dimensionless),

and D^{ω} is the liquid transport coefficient in m^2/s.

So, in EnergyPlus is where the hygrothermal properties of the earth construction and the rest of materials included in the model have been introduced, changed and studied. The hygrothermal properties for all the materials have been extracted from the WUFI 2D-3 database [29]. WUFI is a software that allows realistic calculation of the transient coupled one- and two-dimensional heat and moisture transport in walls and other multi-layer building components exposed to natural weather, but for this study just the database has been used.

In EnergyPlus is also where the desired variable outputs have been selected. In this case are the annual heating and cooling consumptions, and temperature and relative humidity inside the house. The relative humidity results are used to check if the established comfort conditions are maintained.

Different types of earths have been simulated to study its effect in the energy consumption: clay loam, silt loam, silty clay loam, and rammed earth stabilized with cement. In the simulations, some of the layers of the exterior walls (specifically the hollow brick partition and the plaster) have been substituted with an earth layer of the same thickness. Changing the materials, as well as changing the type of earth, causes a change of the thermo-physical properties like conductivity and thermal capacity, and in the hygroscopic properties of the wall (capacity for absorption and desorption of water).

When the optimal type of earth has been selected, the temperature and water content profile of one of the walls has been obtained to better understand its behavior and the effect of the earth layer.

Also, a parametric study has been carried out varying the thickness of the earth layer, with the optimal type of earth, to see its effect in the energy consumption. The parametric analysis has been achieved using JEPlus [30], since it is able to achieve multiple simulations changing a specific variable within a given range.

The methodology and interaction between the different tools is illustrated in figure 4.

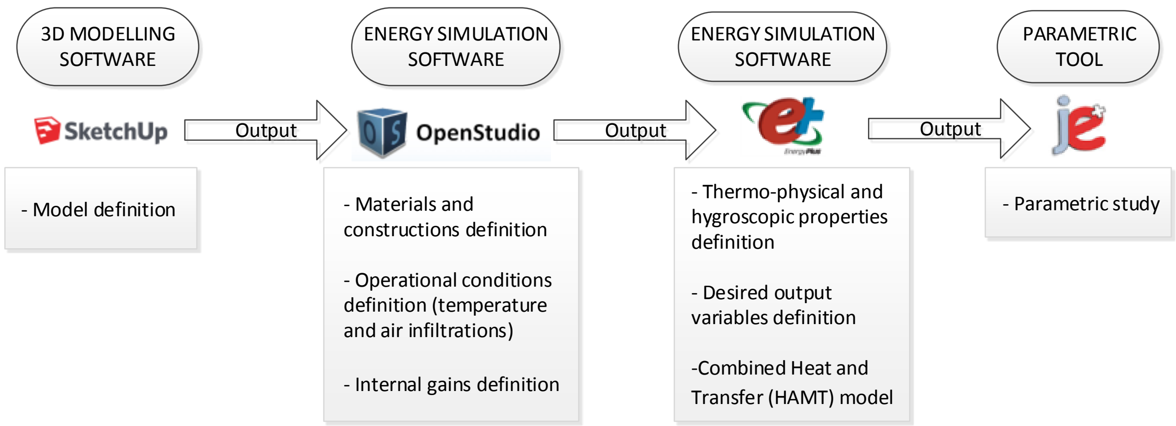

Figure 4. Methodology and interaction between the programs.

3.2 Energy consumption and economic evaluation

The annual heating and cooling energy demand has been obtained by the sum of the monthly energy demand of the individual thermal zones. Then, to obtain the electricity consumption (W) associated to heating and cooling, the energy demand (|Q|) has to be divided by the COP, that has been considered 3 [21], following equation (3).

$$COP = \frac{|Q|}{W} = 3 \tag{3}$$

To obtain the annual cost, the annual consumption has been multiplied by the actual price of electricity, which is 0.229 €/kWh [31].

Having the annual electricity consumption, it has also been calculated the cost in 20 and 50 years with equation (4) and having considered that every year the cost of electricity increases by 5%.

$$Cost_{elec\_n} = \sum_n Consump_{elec} \cdot PCost_{elec} \cdot (1 + Inf)^n \tag{4}$$

Where:

n is the number of years,

$Cost_{elec\_n}$ is the electricity cost for n years in €,

$Consump_{elec}$ is the annual electricity consumption in kWh,

$PCost_{elec}$ is the actual cost of electricity in €/kWh,

and Inf is the electricity cost inflation.

3.3 Environmental impact

To quantify the difference in the environmental impact, a LCA has been carried out. This has been done in order to quantify and compare the impact of the materials and the energy consumption of the base case and the case with earth construction. The environmental impacts have been measured with the Eco-indicator impact point given by ReCiPe Endpoint (H,A), extracted from the database EcoInvent v3.2 [32].

The materials have been searched through the filter "market", which includes extraction, transformation and transport. For the case of the hollow brick partition and the plaster, the market waste has also been included, to take into account the waste treatment impact from the rehabilitation.

The impacts are divided into three categories: ecosystem quality, human health and resources.

The material's impact has been obtained with equation (5).

$$Total_{impact\_mat} = \sum impact_{mat} \cdot Mass \tag{5}$$

Where:

$Total_{impact\_mat}$ are the total impact points associated to the materials,

$impact_{mat}$ is the impact of each material in points/kg,

and Mass is the amount of each material in kg.

The electricity consumption impact during n years has been obtained with equation (6).

$$Total_{impact\_elec} = impact_{elec} \cdot Consump_{elec} \cdot n \tag{6}$$

Where:

$Total_{impact\_elec}$ are the total impact points associated to electricity consumption,

$impact_{elec}$ is the impact of of the electricity consumption in points/kWh,

$Consump_{elec}$ is the annual electricity consumption in kWh,

and n is the number of years.

The total environmental impact during n years has been obtained by the sum of the materials impact and the electricity consumption impact, following equation (7).

$$Total_{impact} = Total_{impact\_mat} + Total_{impact\_elec} \tag{7}$$

4 Case study

4.1 Location and climatic conditions

The building is assumed to be located in the region of Lleida (Spain), in the climate zone D3, according to the Basic Document of Energy Saving [33]. According to the Köppen climatic classification, Lleida has a cold steppe climate [34]. Winters are humid and cold, and summers are warm. It is not unusual that during the year temperatures can fall under zero degrees in winter and achieve high temperatures (sometimes above 40ºC) in summer. Day and night temperatures present really important oscillations, with similar contrast as summer and winter. This contrast exists because the coastal influence that would soften the difference does not reach this area. Figure 5 shows the location of Lleida.

Figure 5. Lleida location in Spain.

4.2 Building description and geometry

The studied building is a two storey's single-family detached house. It has been designed to be generic enough to represent the building typology of single-family detached housing from 1960-1979. Construction elements and materials have been chosen as representative for this building typology.

The building is supposed to be placed on a flat and open terrain without surrounding obstacles. The house footprint is 6.45 m × 8.45 m. Each floor's height is 2.8 m and the roof has a 20% slope. Each floor has a heated floor area of 47 m^2, giving a total area of 94 m^2. The total window area is 14.55 m^2, which gives a windows-to-floor area ratio of 15.48%. Figure 6 shows the interior distribution of the house. The main façade is oriented to the south.

Figure 6. First floor distribution (left) and second floor distribution (right) of the building.

Table 2 shows the net area and volume of each room of the house.

Table 2. Net area and volume of the rooms.

Room	Floor	Net area (m^2)	Volume (m^3)
Kitchen	1	7.64	21.38
Living-room	1	34.17	95.68
Bathroom 1	1	5.17	14.49
Bedrooms	2	41.81	146.43
Bathroom 2	2	5.17	15.65
Total	**2**	**93.96**	**293.63**

4.3 Construction elements

Construction elements have been selected from the CTE [35] as representative from the selected period for single-family detached housing in Spain. A diagram and the materials from each one of the construction elements chosen are shown in the following sections.

4.3.1 Exterior walls

The exterior walls are formed by a layer of perforated brick, a non-ventilated chamber, a hollow brick partition, and a layer of plaster in the interior. The elements that form the exterior walls and their thickness (in mm) are shown in figure 7.

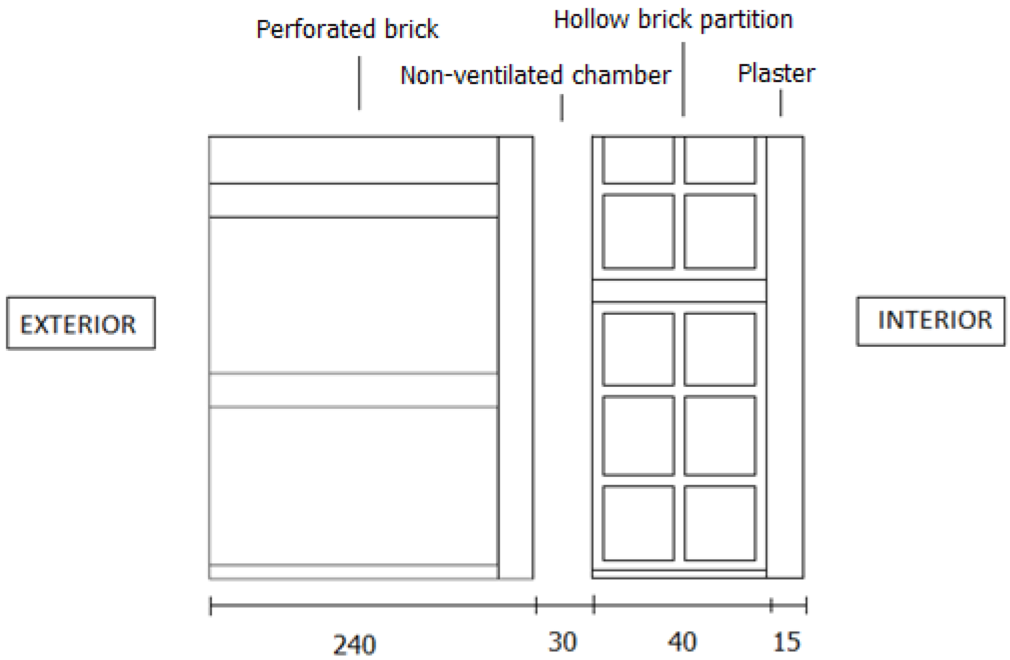

Figure 7. Exterior wall elements diagram [35].

4.3.2 Interior walls

The interior walls are formed by a layer of hollow bricks with a layer of plaster at both sides. A diagram of the elements that form the interior walls and their thickness (in mm) is shown in figure 8.

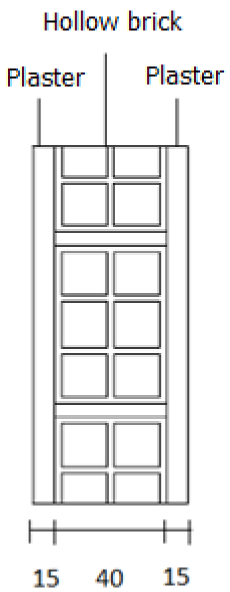

Figure 8. Interior wall elements diagram [35].

4.3.3 Foundation

The foundation is formed by a layer of concrete with light aggregates with a layer of cement mortar for masonry on top of it. The floor tiles have not been taken into account in this study. A diagram of the elements that form the foundation and their thickness (in mm) is shown in figure 9.

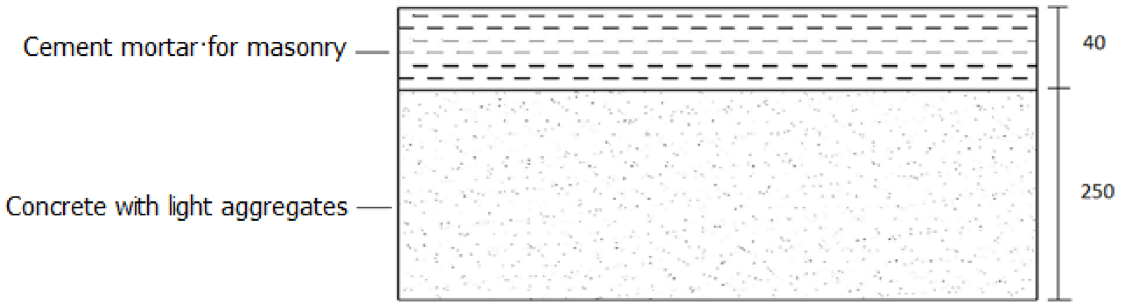

Figure 9. Foundation elements diagram.

4.3.4 Interior ceiling

The interior ceiling is formed by a layer of cement mortar for masonry, an unidirectional ceramic beam and a layer of plaster. A diagram of the elements that form the interior ceiling and their thickness (in mm) is shown in figure 10.

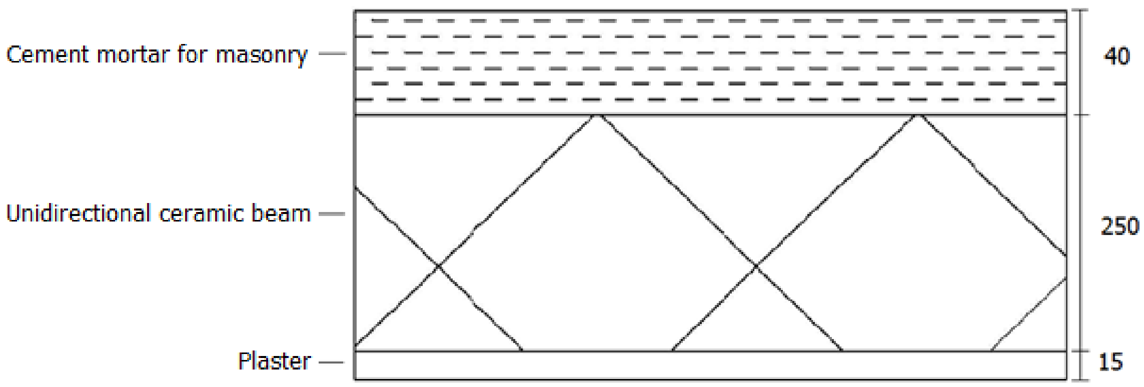

Figure 10. Interior ceiling elements diagram.

4.3.5 Roof

The roof is formed a layer of baked clay roof tiles, an unidirectional ceramic beam and a layer of plaster in the interior. The elements that form the roof and their thickness (in mm) are shown in figure 11.

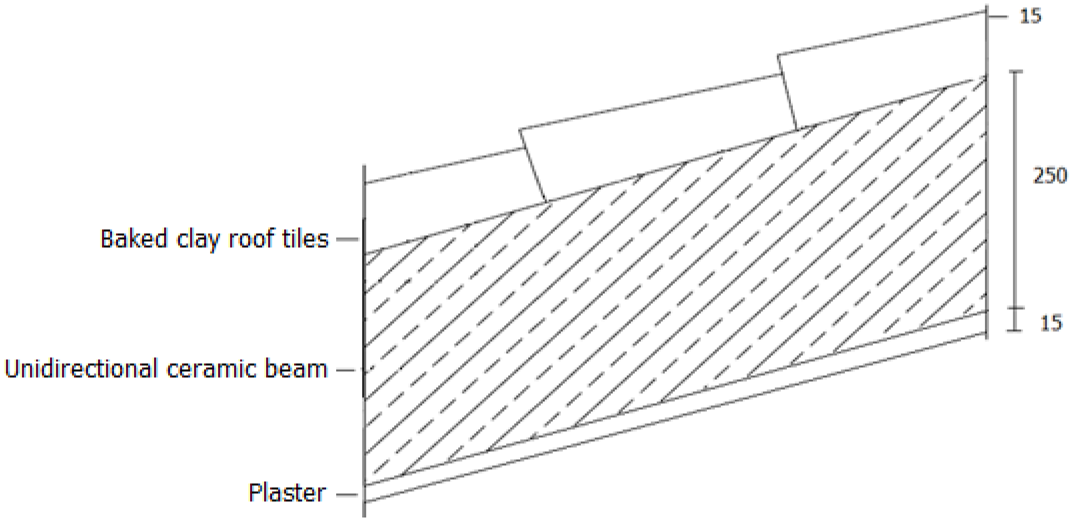

Figure 11. Roof elements diagram [35].

4.3.6 Windows and doors

The windows are formed by 6mm single glazing with wooden frames and the doors are made of oak. The exterior doors are 70 mm thick and the interior doors are 40 mm thick.

4.4 Model design

As explained in the introduction, the building has been designed with Google Sketchup. The isometric views of the model are shown in figure 12.

To facilitate the model design, and the posterior simulations, some simplifications have been carried out. The stairs from the first to the second floor have been modeled as a hole and the bedrooms have been modeled as only one room. Also, the house has a terrace in the second floor that has been modeled as a shadow element, as shown in figure 12, since the only condition that affects the study is the shadow it casts on the corresponding portion of the first floor outside walls.

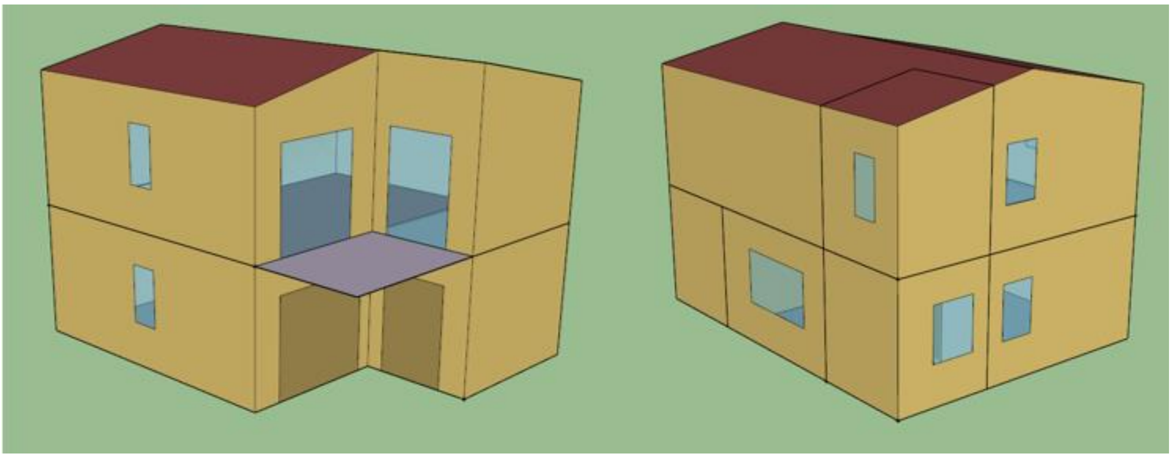

Figure 12. Isometric frontal (left) and rear (right) view of the building model.

Five different thermal zones have been assigned, corresponding to the existing rooms and taking into account the simplification of the bedrooms, which are:

- Thermal zone 1: Kitchen.
- Thermal zone 2: Living-room.
- Thermal zone 3: Bathroom 1 (first floor).
- Thermal zone 4: Bedrooms.
- Thermal zone 5: Bathroom 2 (second floor).

4.4.1 Thermal bridges

A thermal bridge is a localized area of the building envelope where the heat flow is different (usually increased) in comparison with adjacent areas, if there is a difference in the temperature between the inside and the outside.

The effect of thermal bridges are: altered (decreased in the heating period) interior surface temperatures and altered (usually increased) heat losses. In the worst case, the decrease in the interior surface temperatures can lead to moisture penetration in building components and mold growth.

Since they can alter temperature and increase heat losses, thermal bridges have been taken into account in the model, and are located in the windows frames, where the roof meets the exterior walls, and where the interior ceiling meets the exterior walls. Since the floor on the ground is not isolated, there is no thermal bridge located there. Figure 13 shows where the thermal bridges have been drawn in the model.

The thermo-physical properties of the thermal bridges (conductivity, density and specific heat) are the same as the wood from the doors, but with the exterior walls thickness (355 mm).

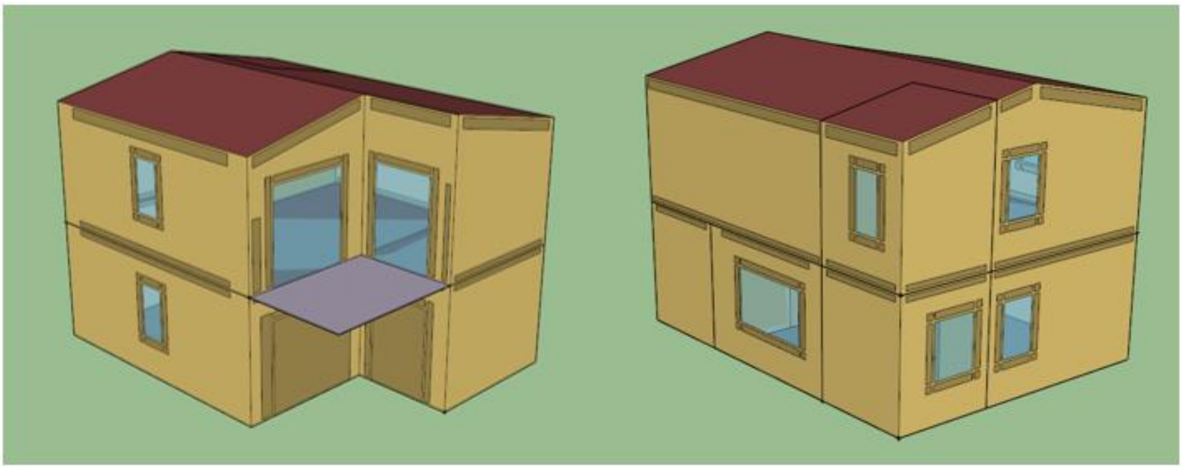

Figure 13. Thermal bridges location in the model.

4.5 Internal gains

The internal gains considered in this study are gains due to the presence of occupants and their activity in each room, lighting and electric equipment.

The physical activity of the house occupants generates heat that has to be taken into account during the simulations. Each room has been assigned with one habitual activity [36], shown in table 3, with the correspondent metabolic rate. Since the metabolic rate has to be introduced as watts per person, the one given in watts per area has been multiplied for the area occupied by an adult person, which is 1.8 m^2/person [36].

Table 3. Activity levels.

Room	**Activity**	**Metabolic rate (W/m^2)**	**Metabolic rate (W/pers)**
Living-room	Seated, quiet	60	108
Kitchen	Cooking	115	207
Bedrooms	Sleeping	40	72
Bathroom	Standing, relaxed	70	126

Occupation gains are calculated by the program, with the activity levels together with the occupation schedule, shown in table 4.

Table 4. Occupation schedule.

	Workday	Weekend
Living-room	8 to 13.59h: 1 15 to 16.59h: 1 17 to 21.59h: 3 22 to 23h: 2 to 24h: 3	8 to 13.59h: 4 14 to 14.59h: 3 15 to 21.59h: 4 22 to 23.59h: 3
Bathroom (x2)	7 to 7.59h: 1 23 to 23.59h: 1	7 to 7.59h: 1 23 to 23.59h: 1
Bedrooms	0 to 6.59h: 3 7 to 7.59h: 4	0 to 6.59h: 3 7 to 7.59h: 4
Kitchen	14 to 14.59h: 1 22 to 22.59h: 1	14 to 14.59h: 1 22 to 22.59h: 1
Total	24 to 6.59h: 4 7 to 15.59h: 1 16 to 22.59h: 3 23 to 23.59h: 4	0 to 24h: 4

The lightning and electric equipment gains values and schedules have been obtained from Annex C of the Basic Document of Energy Saving [24], and are shown in table 5.

Table 5. Lightning and electric equipment gains.

	1-7h	8h	9-15h	16-23h	24h
Lightning (W/m^2)					
Workday, weekday and holiday	0.44	1.32	1.32	1.32	2.2
Equipment (W/m^2)					
Workday, weekday and holiday	0.44	1.32	1.32	1.32	2.2

4.6 Comfort conditions

The comfort conditions specified in the simulations are the temperature set-point and the ventilation (or infiltration) rate. The required values have been obtained from Annex C of the Basic Document of Energy Saving [24]. The temperature set-points are shown in table 6 and ventilation rate schedule are shown in table 7.

Table 6. Temperature set-point schedule.

	1-7h	8h	9-15h	16-23h	24h
High Temperature Set-point (ºC)					
January to May	-	-	-	-	-
June to September	27	-	-	25	27
October to December	-	-	-	-	-
Low Temperature Set-point (ºC)					
January to May	17	20	20	20	17
June to September	-	-	-	-	-
October to December	17	20	20	20	17

Table 7. Ventilation rate schedule.

	1-7h	8h	9-15h	16-23h	24h
Summer ventilation (ren/h)					
Workday, weekday and holiday	4	4	0.51	0.51	0.51
Winter ventilation (ren/h)					
Workday, weekday and holiday	0.51	0.51	0.51	0.51	0.51

The infiltrations rate (except in summer from 1 to 8.59h), is the minimum flow required by the DB HS [37] and has been calculated. The data required for the calculations is shown in table 8.

Table 8. Minimum ventilation flow.

Rooms	Nº	Minimum ventilation flow required q_v (l/s)	
		For occupant	Total
Double bedroom[1]	2	4 occupants · 5 l/s	20 (Impulsion)
Living-room	1	4 occupants · 3 l/s	12 (Impulsion)
Bathroom	2	15 per room	30 (Extraction)
Kitchen	1	2 · 5.81 m²	11.62 (Extraction)

Which results in an impulsion flow of 32 l/s and an extraction flow of 41 l/s, and being the extraction flow the higher one:

$$Q_V = 41.62L/s \frac{1m^3}{1000L} \frac{3600s}{1h} = 149.8m^3/h \quad (8)$$

[1] Is considered a double bedroom when the area is higher than 8 m^2.

The minimum ventilation flow in renovations per hour is:

$$Q_{ren\_h} = \frac{Q_V}{V_{build}} = \frac{149.8m^3 / h}{293.6m^3} = 0.5103 \, {}^{renovations}\!/_{hour} \quad (9)$$

4.7 Material parameters

As mentioned in the introduction, the hygroscopic properties for all the materials required for the simulations have been extracted from the WUFI 2D-3 database [29]. The database contains a limited number of materials, so it has been necessary to look for similar materials to the ones listed in section 4.3. In some cases this has proven to be difficult, as can be observed in table 9. This table shows a comparative of the materials from the CTE [35] and the materials chosen from the WUFI database and their thermo-physical properties. The hygroscopic properties are shown in annex 1.

Table 9. Comparison between chosen materials and WUFI materials properties.

Property	Material CTE	CTE value	Material WUFI	WUFI value
ρ (kg/m³)	Perforated brick	770	Brick (old) (North America database)	1670
Porosity (m³/m³)		-		0.196
Cp (J/kg·K)		1000		840
k (W/m·K)		0.32		0.4 - 0.776
μ (dimensionless)		10		16 - 4.95
ρ (kg/m³)	Hollow bricks	1000	Brick (old) (North America database)	1670
Porosity (m³/m³)		-		0.196
Cp (J/kg·K)		1000		840
k (W/m·K)		0.445		0.4 - 0.776
μ (dimensionless)		10		16 - 4.95
ρ (kg/m³)	Hollow brick partition	780	Brick (old) (North America database)	1670
Porosity (m³/m³)		-		0.196
Cp (J/kg·K)		1000		840
k (W/m·K)		0.35		0.4 - 0.776
μ (dimensionless)		10		16 - 4.95
ρ (kg/m³)	Unidirectional ceramic beam	1220	Clay (North America database)	1267
Porosity (m³/m³)		-		0.517
Cp (J/kg·K)		1000		850
k (W/m·K)		0.89		0.288 - 1.7253
μ (dimensionless)		10		50
ρ (kg/m³)	Concrete with light aggregates	1900	Concrete (MASEA database, Germany)	2104
Porosity (m³/m³)		-		0.22
Cp (J/kg·K)		1000		776
k (W/m·K)		1.35		1.373 - 2.522
μ (dimensionless)		60		76

Table 9 (cont.). Comparison between chosen materials and WUFI materials properties.

Property	**Material CTE**	**CTE value**	**Material WUFI**	**WUFI value**
ρ (kg/m^3)	Cement or lime mortar for masonry	2100	Concrete w/c 0,7 (LTH Lund University, Sweden)	2275
Porosity (m^3/m^3)		-		0.16
Cp (J/kg·K)		1000		850
k (W/m·K)		1.8		1.7
μ (dimensionless)		10		147 - 0.625
ρ (kg/m^3)	Plaster	1100	Interior plaster (Fraunhofer-IBP)	850
Porosity (m^3/m^3)		-		0.65
Cp (J/kg·K)		1000		850
k (W/m·K)		0.57		0.2 - 1.424
μ (dimensionless)		6		8.3
ρ (kg/m^3)	Backed clay roof tiles	2000	Red Matt Clay Brick (North America database)	1935
Porosity (m^3/m^3)		-		0.217
Cp (J/kg·K)		1000		800
k (W/m·K)		0.57		0.495
μ (dimensionless)		30		137.8 - 96.8
ρ (kg/m^3)	Oak Wood	710	Oak old (MASEA database, Germany)	740
Porosity (m^3/m^3)		-		0.35
Cp (J/kg·K)		1600		1400
k (W/m·K)		0.18		0.1522 - 0.245
μ (dimensionless)		50		223

4.8 Definition of design alternatives

First, the base case has been simulated to obtain the results without changing the structure of the exterior walls, shown in figure 7. Then, for the rest of the cases, the layers of hollow brick partition and plaster have been substituted for an earth layer of the same thickness (55 mm), as shown in figure 14.

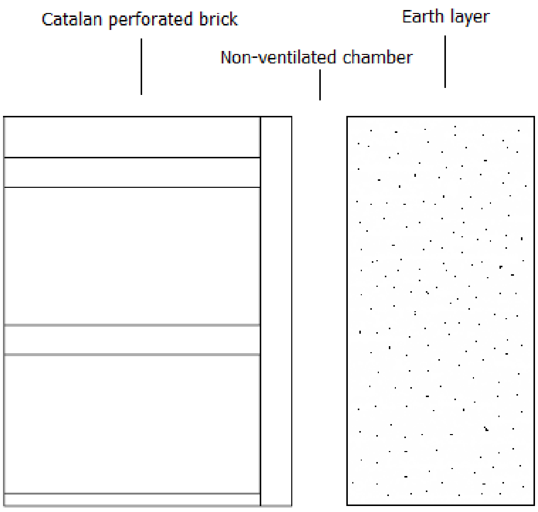

Figure 14. Exterior wall structure with earth.

Four different types of earth have been simulated: three are types of unstabilized rammed earth and one is rammed earth stabilized with cement. The cases simulated are:

- Case 1: base case.
- Case 2: exterior walls with clay loam.
- Case 3: exterior walls with silt loam.
- Case 4: exterior walls with silty clay loam.
- Case 5: exterior walls with stabilized rammed earth.

4.9 Earth composition sensibility test

The unstabilized types of earth are sorted by their percentage of clay, sand and silt with the soil texture triangle shown in figure 15, where the three chosen types of unstabilized earth are marked. The thermo-physical and hygroscopic properties of the simulated types of earth are shown in annex 2.

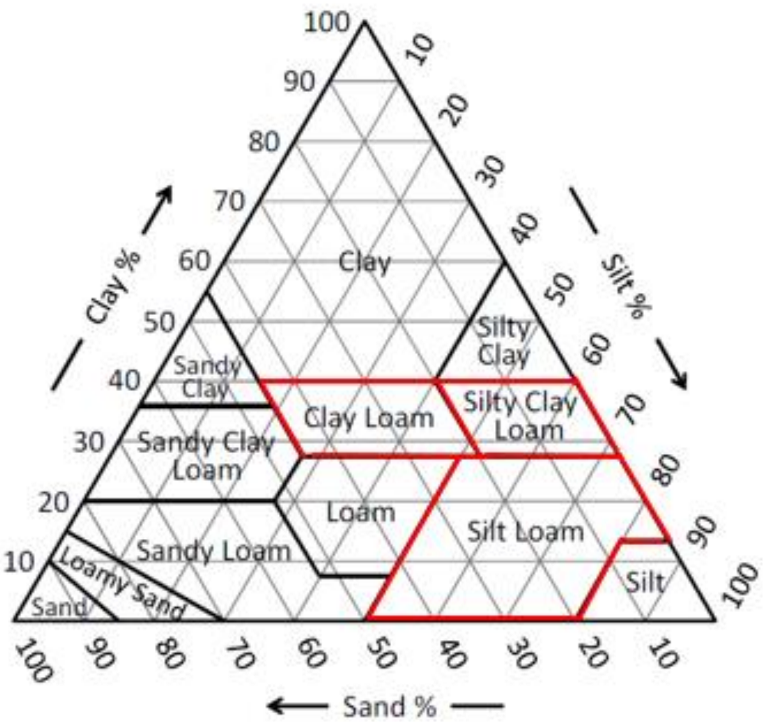

Figure 15. Soil texture triangle [38].

Unlike the rammed earth stabilized with cement, the composition of which is ironstone waste (2/3 volume), sand (1/3 volume) and cement (7wt%) [17], the unstabilized types of earth do not have a specific composition, but a range, as can observed in figure 15. To obtain the environmental impact, it is necessary to have the mass of every component. So for the case of unstabilized earth, a sensibility analysis has been carried out to check the magnitude of the effect of composition on the environmental impact points. It has been done with 3 different compositions of silty clay loam, shown in table 10. The effect is shown in figure 16.

Table 10. Compositions of the sensibility test.

Composition	Clay (%)	Sand (%)	Silt (%)
1	35	10	55
2	27	20	53
3	40	20	40

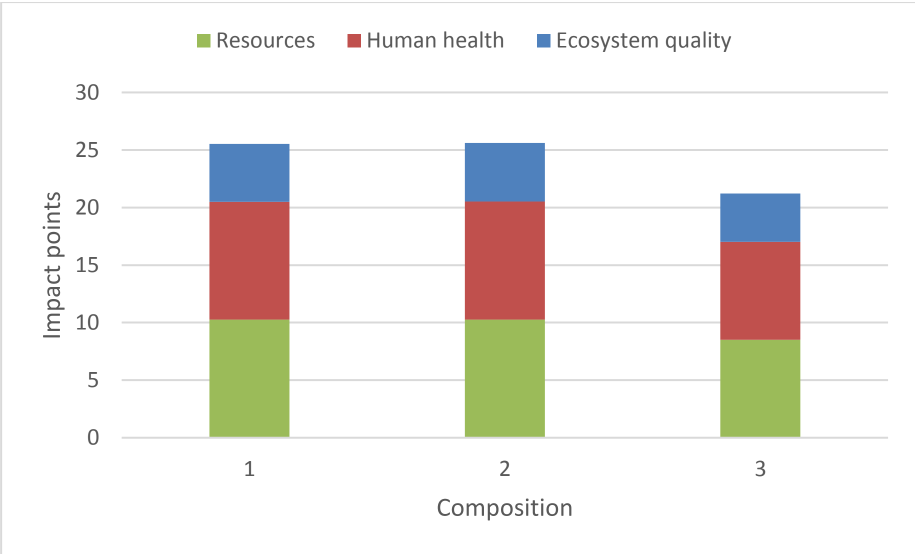

Figure 16. Effect of earth composition in the environmental impact points.

As can be observed in figure 16, the effect of the composition in the environmental impact points is small, so the first composition has been selected from table 10 to represent the whole range.

5 Results and discussion

5.1 Energy consumption

Table 11 shows the annual heating and cooling demand resulting of the simulations of all the cases specified in section 4.8 and the total annual energy demand.

Table 11. Annual heating and cooling energy demand.

Case		Heating demand (kWh)	Cooling demand (kWh)	Total energy demand (kWh)
1	Base case	8750	1099	9849
2	Clay loam	8697	1135	9832
3	Silt loam	8714	1127	9841
4	Silty clay loam	8640	1139	9779
5	Stabilized rammed earth	9032	1102	10134

Observing the results from table 11, the annual consumption does not change a great deal when changing the layers of hollow brick partition and plaster for an earth layer in cases 2 to 4, but still the total consumption is reduced even though refrigeration increases slightly. The fact that refrigeration increases may be due to lack of ventilation during the night, when the heat stored in the walls is released. Despite that, since the ventilation rate in this study is bound to the comfort conditions established, it would have to be studied further. In case 5, using stabilized rammed earth actually increases heating and refrigeration consumption, and so this type of earth is discarded for further tests.

From cases 2 to 4 the best option is the silty clay loam, which reduces energy consumption the most, even though the difference is minimal. Nonetheless, the rest of tests have been done using silty clay loam.

It has to be taken into account that no other measures apart from the substitution of materials in some of the external walls' layers has been applied. Only hygroscopic and thermal properties of the material modification have been considered, so changes are small. The effect of introducing earth construction applying at the same time other substantial measures like change of glazing and addition of insulation would have to be studied to see an increased effect in the energy reduction.

A parametric study has been carried out varying the silty clay loam layer's thickness to see the effect in energy consumption, and the thickness range covered goes from 0.055 m to 0.11 m. Figure 17 shows the heating and cooling demand results respectively for all the thickness range.

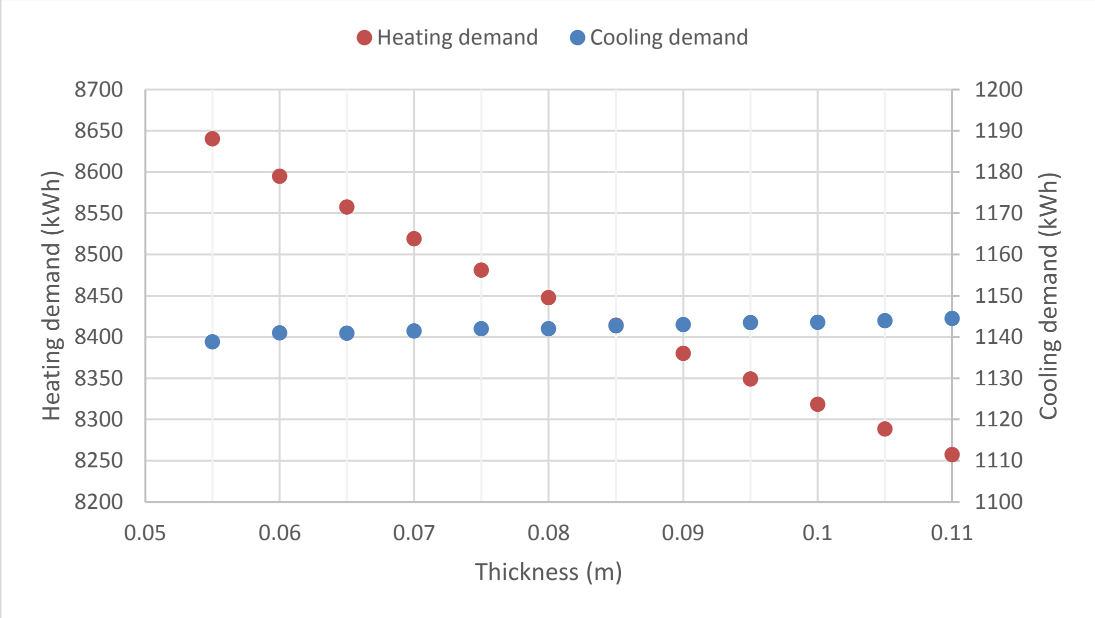

Figure 17. Energy demand results from the parametric study.

As can be observed in figure 17, the heating demand has a decreasing tendency while increasing the earth layer's thickness, but the cooling demand has a slightly opposed tendency and increases with increasing thickness. Even if the cooling demand increases, the total consumption results decreases while increasing the thickness. This happens due to the reduction in heating demand by a 4% while refrigeration only increases by a 0.4%.

5.2 Cost evaluation

Table 12 shows the comparison of the cost of the electricity consumption associated to the heating and cooling energy demand for the first year, in 20 years and in 50 years of the base case and the silty clay loam case. Results take into account the increasing cost of energy due to inflation.

Table 12. Cost evaluation results.

Case	**Annual electricity consumption (kWh)**	**Cost (€)**		
		1 year	**20 years**	**50 years**
Base case	3283	752	23,681	86,268
Silty clay loam	3260	746	23,514	85,658

Observing the results shown in table 12, it can be seen that, even in the long term, cost reduction is minimal. Given that the reduction in energy consumption and cost is so small, the cost of rehabilitation would not be justified, but it could still be considered as an alternative for new construction.

The cost evaluation has also been done for the energy consumption results of the parametric study. The annual energy consumption and the first year's cost are shown in figure 18. The cost in 20 and 50 years is shown in figure 19.

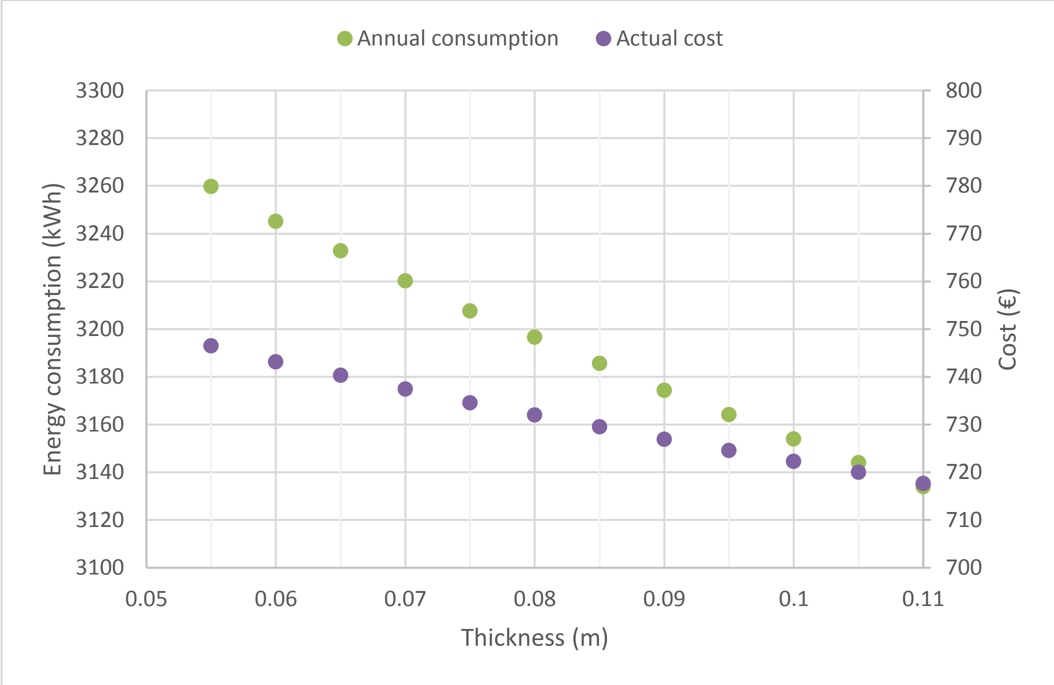

Figure 18. Parametric study results of energy consumption and first year's cost.

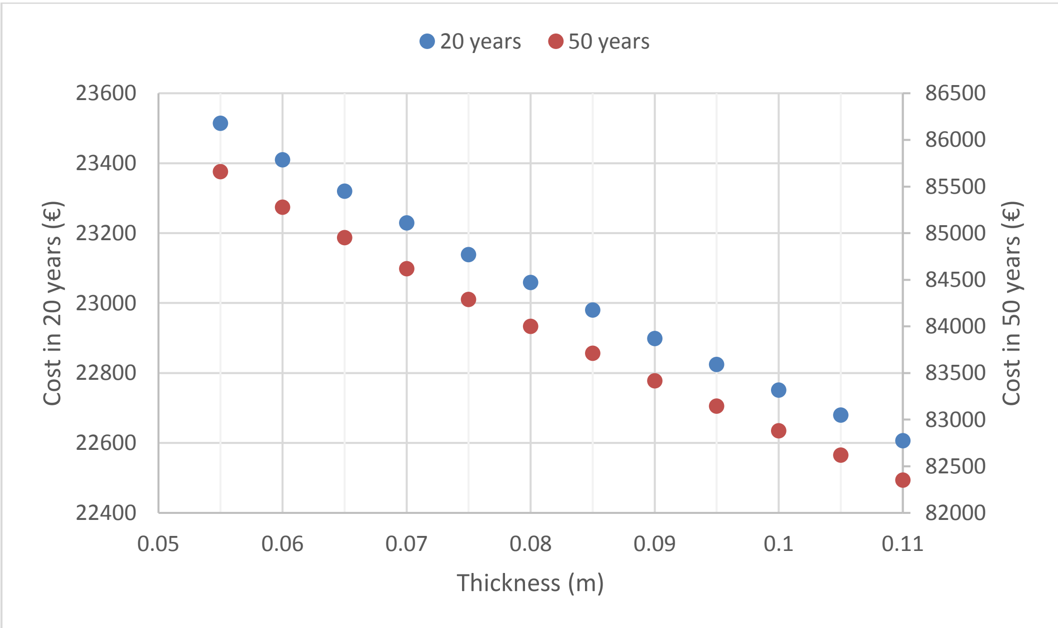

Figure 19. Parametric study cost evaluation in 20 and 50 years.

As shown in figures 18 and 19, the effect of increasing the earth layer's thickness is almost inappreciable in the energy consumption cost of the first year, but it increments when analyzing the cost in 20 and 50 years due to the increasing cost of energy, saving approximately 3000€ in 50 years.

Construction costs have not been evaluated in this study, but earth construction is labor intensive and, in developed countries, labor represents the most part of the construction cost, while the materials increment don't represent an important impact in cost. For that reason, increasing the thickness of the earth layer would be cost efficient in terms of construction, considering at the same time the obtained reduction in energy consumption.

5.3 Comfort conditions

The comfort conditions results that have been reviewed are the temperature and the relative humidity inside the house. The temperature depends on the set-point, and so the results being inside parameters is indicative of the correct performance of the simulations, but the earth effect in the relative humidity does not depend of a set-point and the difference between the cases has been studied.

5.3.1 Temperature

Figure 20 shows the temperature profile of all thermal zones during the year. Since the temperature depends on the set-point input in the simulations (shown in section 4.6), the profile is the same for all the cases and is inside of the comfort conditions.

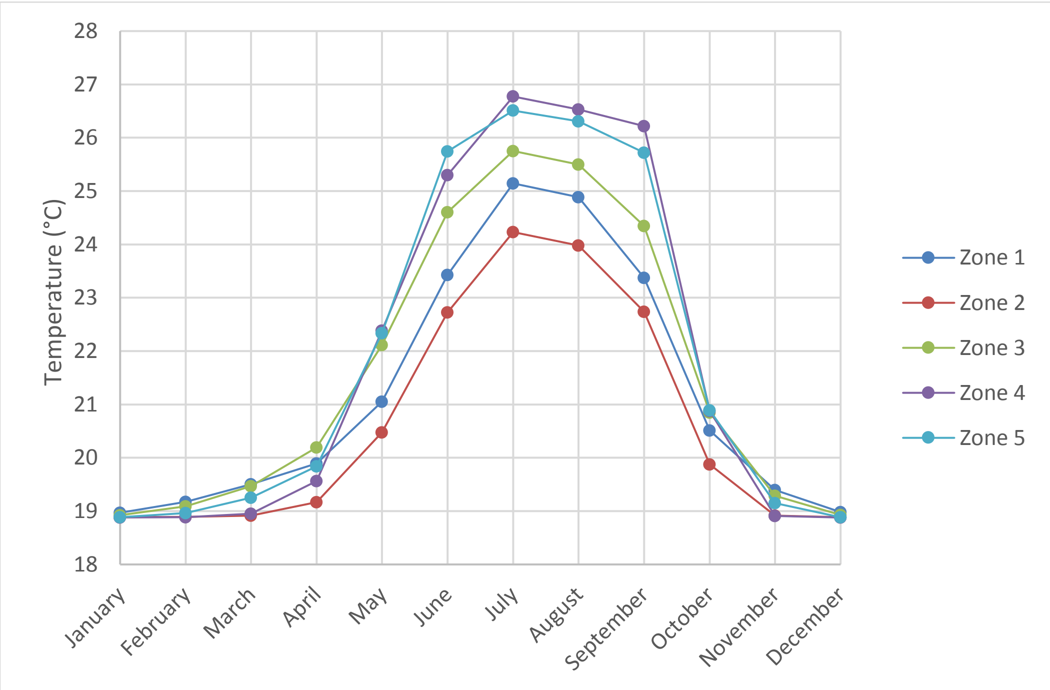

Figure 20. Annual temperature profile.

As can be observed from figure 20 from June to September temperature do not reach the set-point (25-27°C) in thermal zones 1, 2 and 3, which correspond to the kitchen, living-room and the first floor bathroom, contrary to zones 4 and 5, corresponding to the bedrooms and second floor bathroom that reach said set-point. This leads to the conclusion that the walls are sufficiently thick so that heat does not reach the interior but on the second floor the roof counteracts the effect of the walls.

5.3.2 Relative humidity

Figures 21 and 22 show the average relative humidity during the year of the base case and the silty clay loam case respectively.

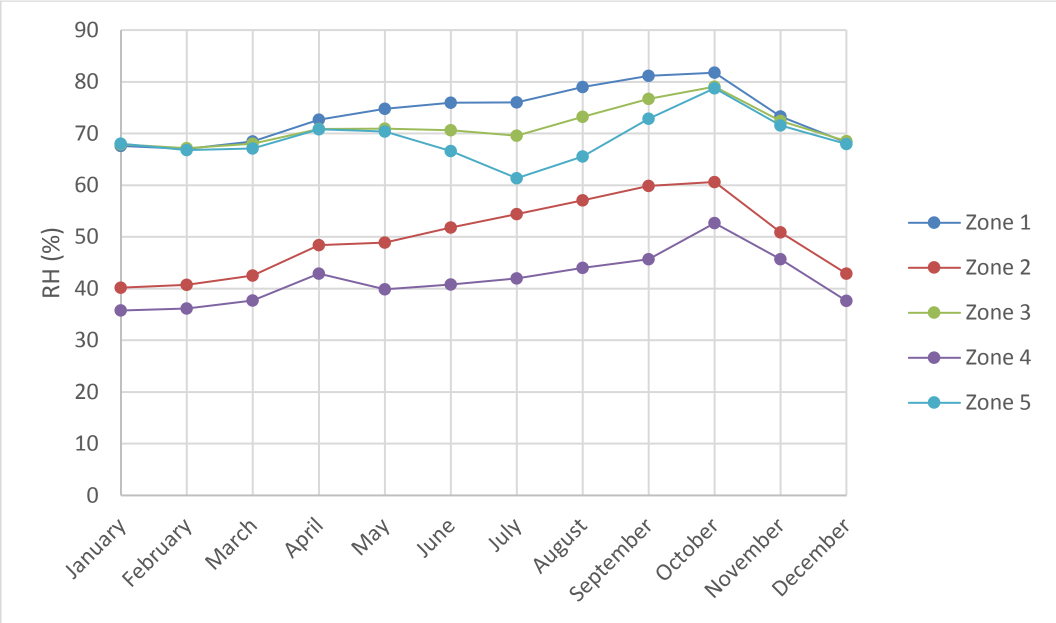

Figure 21. Base case relative humidity results.

As can be observed in figure 21 the relative humidity ranges are divided in 2 groups of zones. Zones 1, 3 and 5 (kitchen and bathrooms) have a relative humidity between 61 and 82%, and zones 2 and 4 (living-room and bedrooms) have a relative humidity between 36 and 61%. The fact that the kitchen and bathrooms have a higher relative humidity range is natural, considering that their area is more reduced than the rest of the rooms.

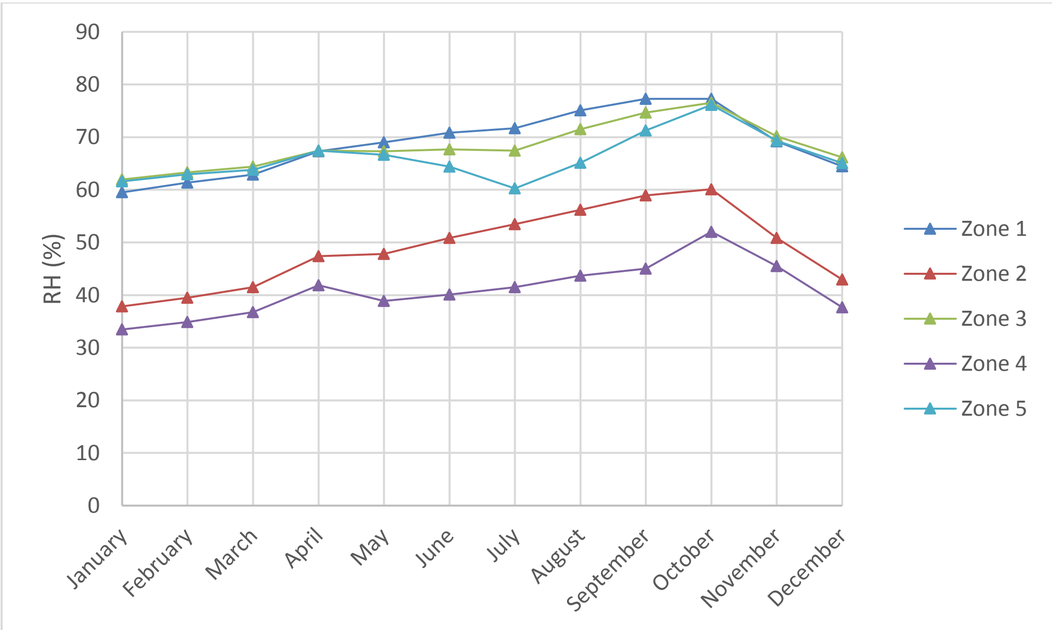

Figure 22. Silty clay loam case relative humidity results

Comparing figures 21 and 22, the tendency in both cases is the same, but earth maintains humidity lower than the base case and slightly smoother.

Taking into account the relative humidity range explained in section 1, the case with silty clay loam maintains a relative humidity lower than 80% at all times, and it is generally below 70% except for thermal zones 1, 3 and 5, which, as said before, it is normal for relative humidity to be higher in those rooms. The lower limit is kept almost the same as the base case. This is illustrated better in figure 23, which shows a comparison of the thermal zones with the higher and the lower limit from both cases.

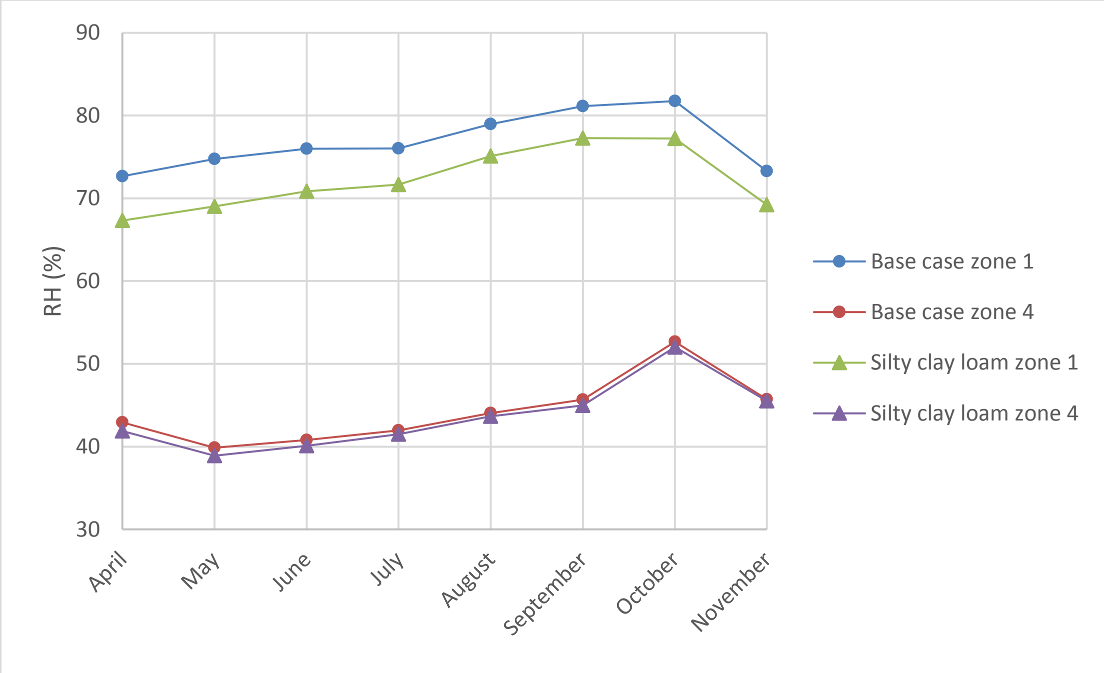

Figure 23. Comparison of the zones with higher and lower relative humidity limits.

The higher limit of the relative humidity is significantly lowered in the silty clay loam case while the lower limit stays almost the same in both cases.

The silty clay loam case has also been simulated doubling the thickness of the earth layer (0.11 m), to see the effect of thickness in the average relative humidity, and the results are shown in figure 24.

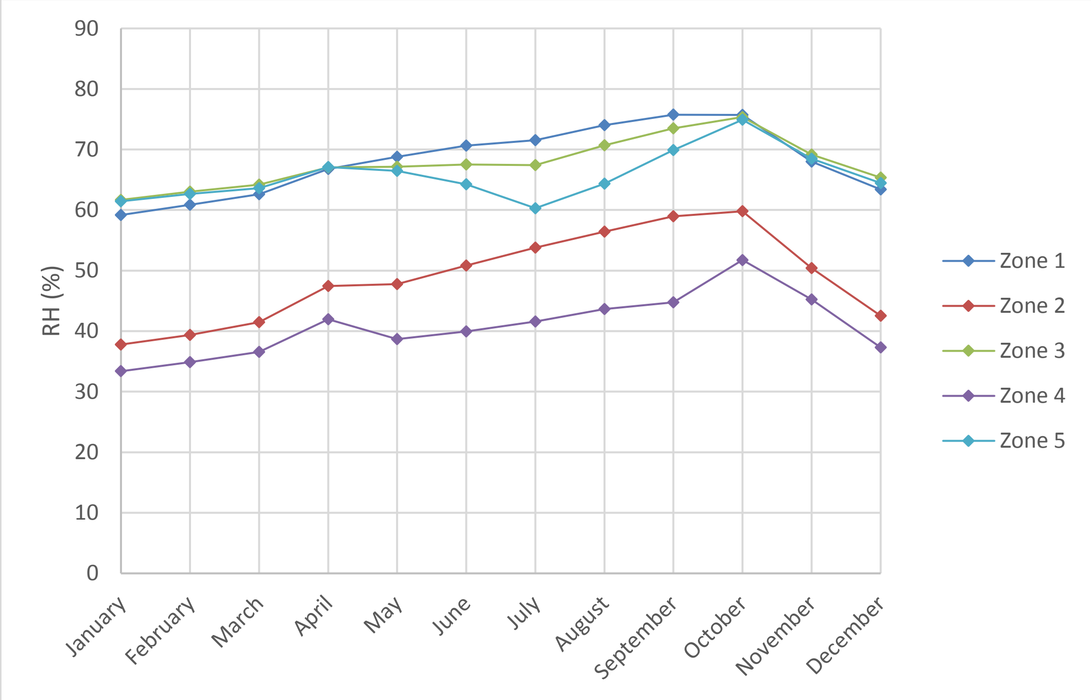

Figure 24. Silty clay loam case relative humidity results doubling the thickness of the earth layer.

Even though it cannot be appreciated in the chart, the relative humidity maximum reduction when doubling the earth layer's thickness is 1.5%. The largest effect observed is obtained by changing the material, the increment of thickness does not affect to the same amount.

5.4 External wall profiles

To calculate the heat and moisture transfer through surfaces the HAMT model splits up surfaces into discrete cells. When reporting profiles of temperature or water content, the data is presented divided by these cells. Each cell is composed of a single material and has a position within the surface. The HAMT model automatically assigns cells to construction objects so that there are more cells closer to boundaries between materials and also at the "surfaces" of the surface. The cell numbering starts from the external surface to the internal surface [39]. The program also gives the origin of every cell, so it is possible to know how the materials are divided.

In the base case, the cells correspond approximately to:

- Cell 1 to 12: perforated brick.
- Cell 13 to 20: non-ventilated chamber.
- Cell 21 to 30: hollow brick partition.
- Cell 31 to 37: plaster.

In the silty clay loam case, the cells correspond approximately to:

- Cell 1 to 12: perforated brick.
- Cell 13 to 20: non-ventilated chamber.
- Cell 21 to 31: silty clay loam.

5.4.1 Temperature profiles

For the temperature profiles, two reference days have been analyzed, one cold day (30th of January) and one hot day (9th of August). Figures 25 and 26 show the temperature profile inside an external wall from the winter day with a time step of 3 hours of the base case and the silty clay loam case respectively.

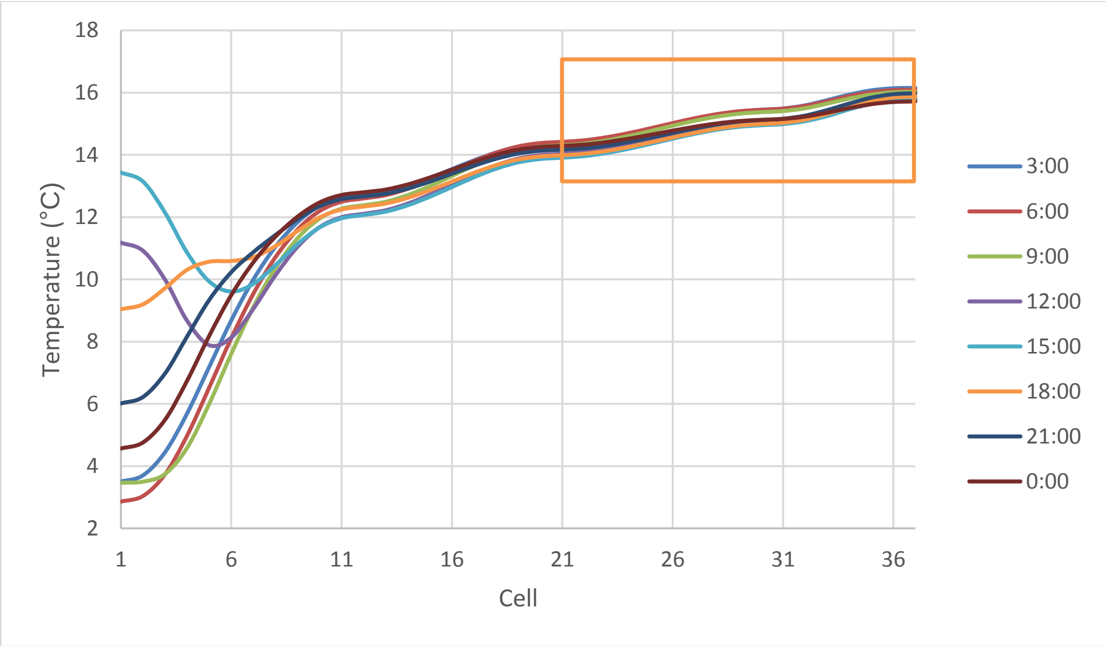

Figure 25. Base case temperature profile inside the external wall from the 30th of January.

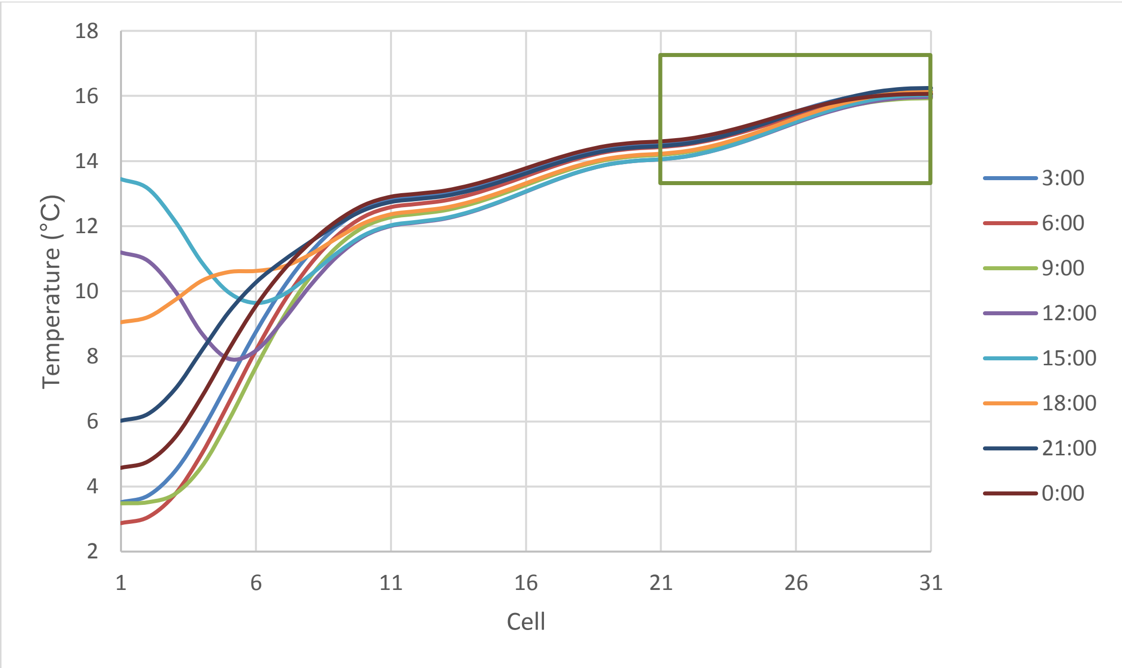

Figure 26. Silty clay loam case temperature profile inside the exterior wall from the 30th of January.

To be able to compare, figure 27 shows a zoom of the cells corresponding to the substituted materials for the 30th of January.

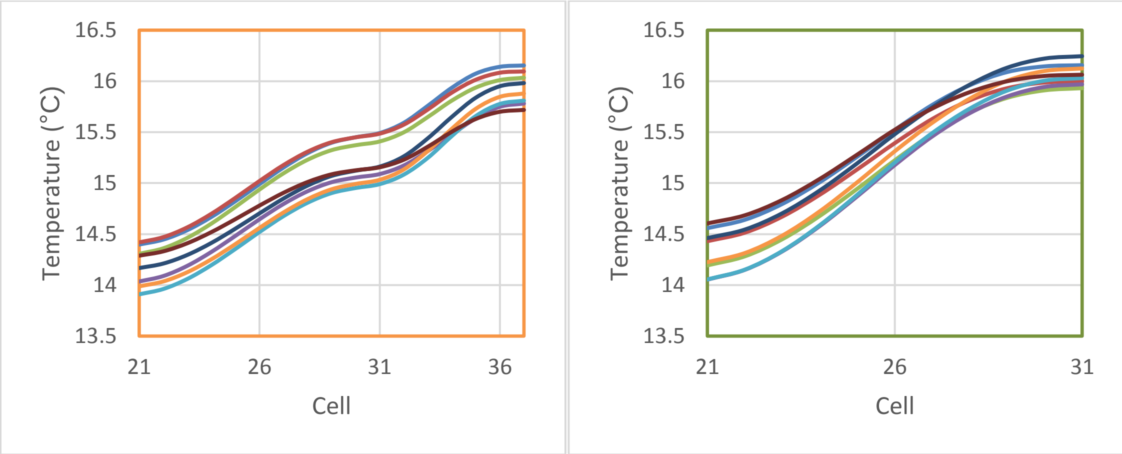

Figure 27. Zoom of the base case (left) and of the silty clay loam case (right) temperature profile from the 30th of January.

As observed in figure 27, although tendency is similar, the silty clay loam maintains temperature smoother through the wall and closer to the set-point than the base case.

Figures 28 and 29 show the temperature profile inside the external wall with the same time step as the figures above from the summer day of the base case and the silty clay loam case respectively.

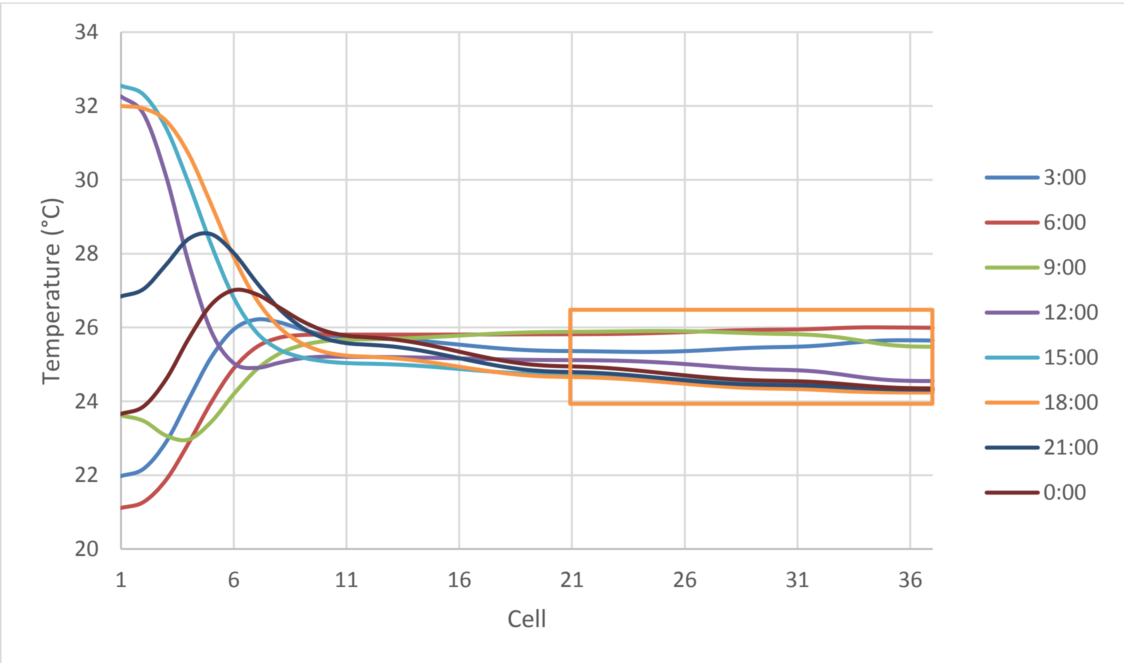

Figure 28. Base case temperature profile inside the exterior wall from the 9th of August.

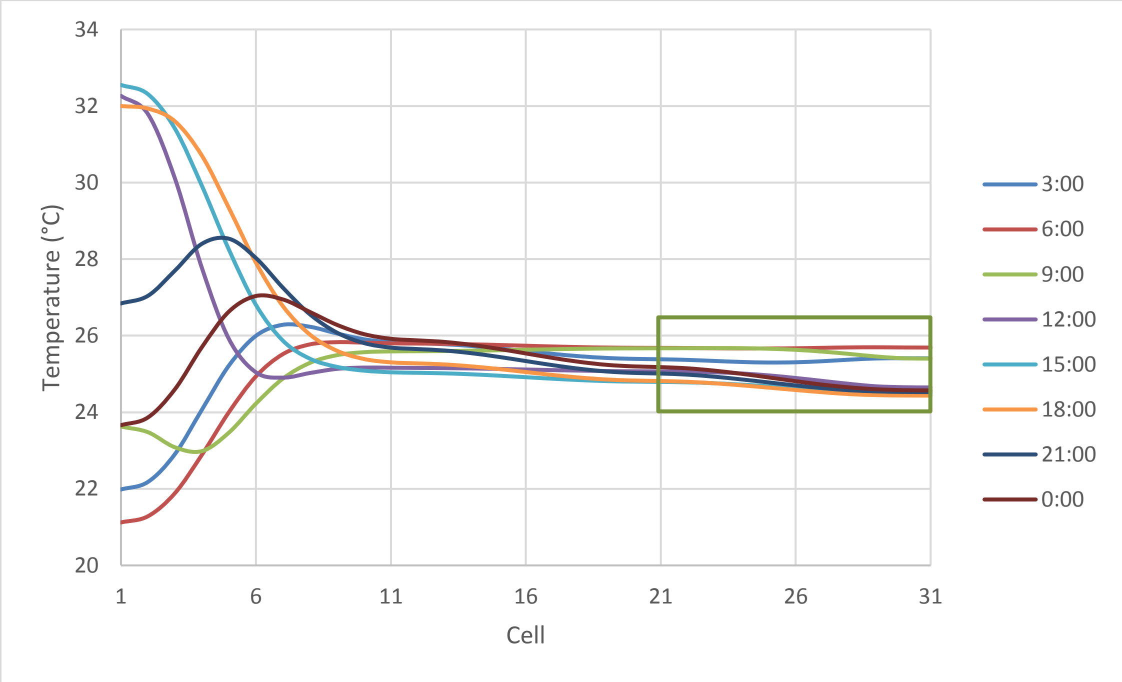

Figure 29. Silty clay loam case temperature profile inside the exterior wall from the 9th of August.

Figure 30 shows a zoom of the cells corresponding to the substituted materials for the 9th of August.

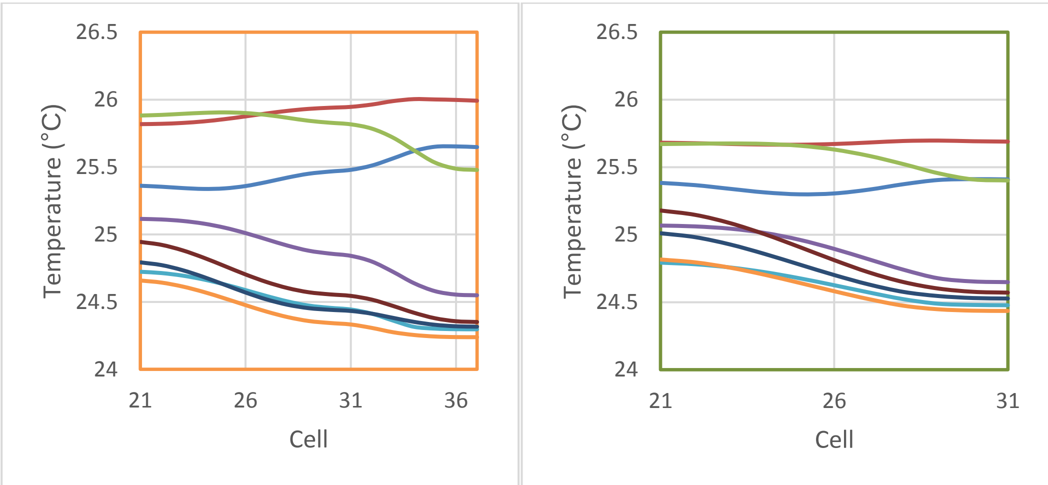

Figure 30. Zoom of the base case (left) and of the silty clay loam case (right) temperature profile from the 9th of August.

As in figure 27, in figure 30 it also can be observed that silty clay loam has a similar tendency as materials in the base case, but it keeps temperature smoother through the wall. In summer though, until 9:00 temperature is lower than the base case, but from 12:00 it is slightly higher. Despite this, it does not reach the set-point, which is 25°C from 16 to 23h and 27°C from 24 to 7h.

5.4.2 Water content profiles

The data represented in the water content profiles corresponds to different hours from different days, with approximately 2 months between each series. The data compared have been extracted from the same days and hours for both cases. The cases have been simulated with an initial water content of 0.01 kg/kg. Figures 31 and 32 show the water content profile of the base case and the silty clay loam case respectively.

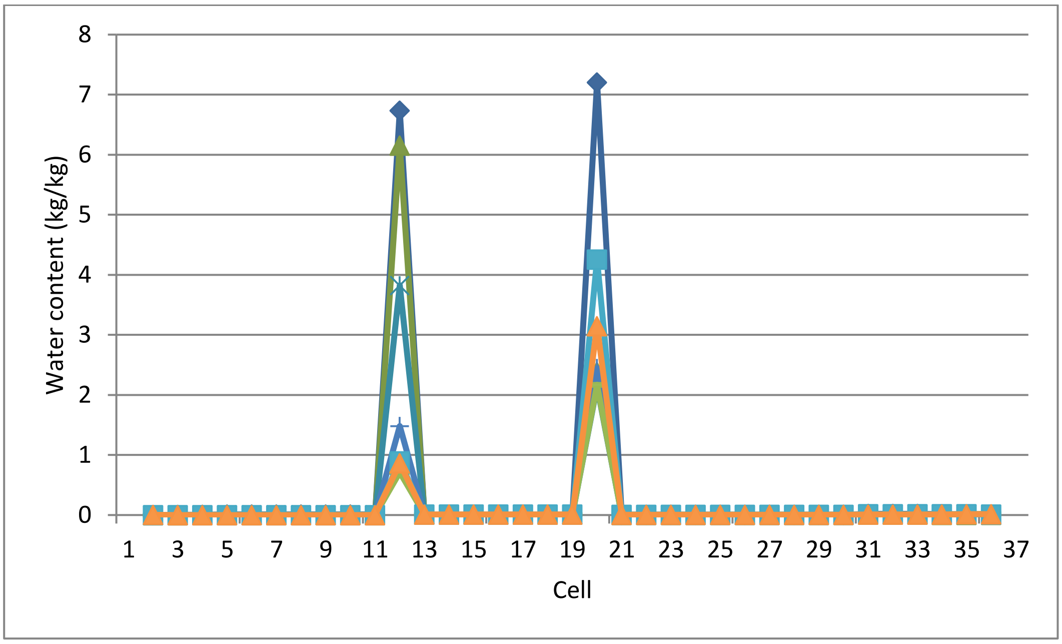

Figure 31. Water content profile inside the external wall of the base case.

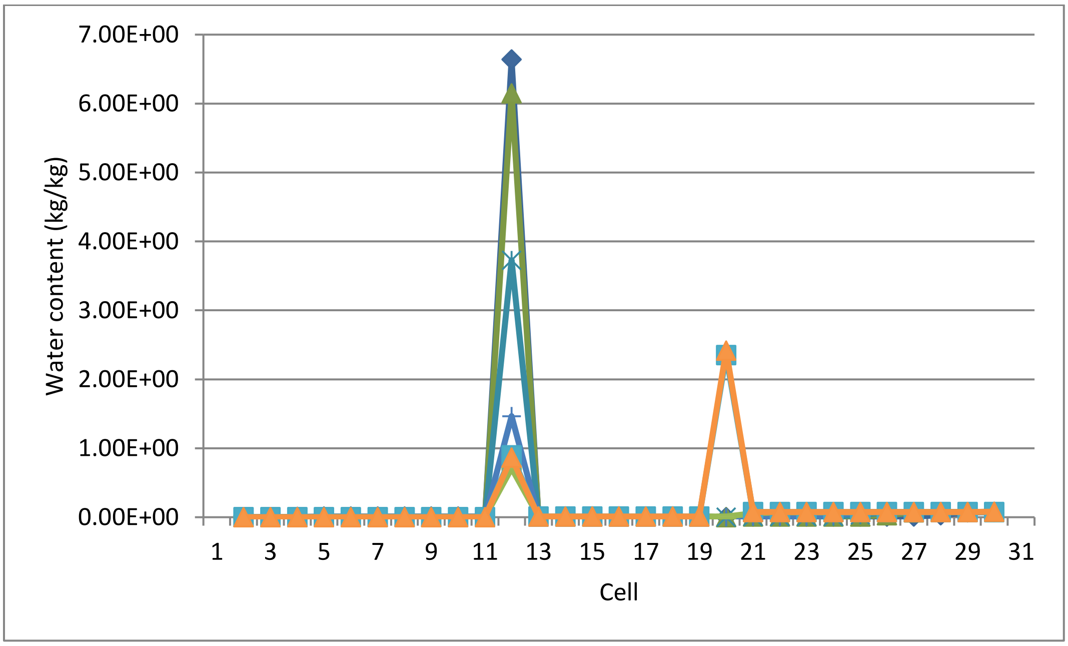

Figure 32. Water content profile inside the external wall of the silty clay loam case.

Figure 31 shows how the water content accumulates in the surfaces in contact with the non-ventilated chamber (cells 13 to 20) on both sides. This is because bricks barely absorb the water contained in the chamber. In figure 32 it can be observed that the same happens on the interior surface of the perforated bricks but not so much on the surface of the earth layer, where more water is absorbed. There are days when no water is accumulated at all, which is better exposed in figure 34.

Figures 33 and 34 show a zoom of the water content profile inside the external wall of the base case and silty clay loam case respectively.

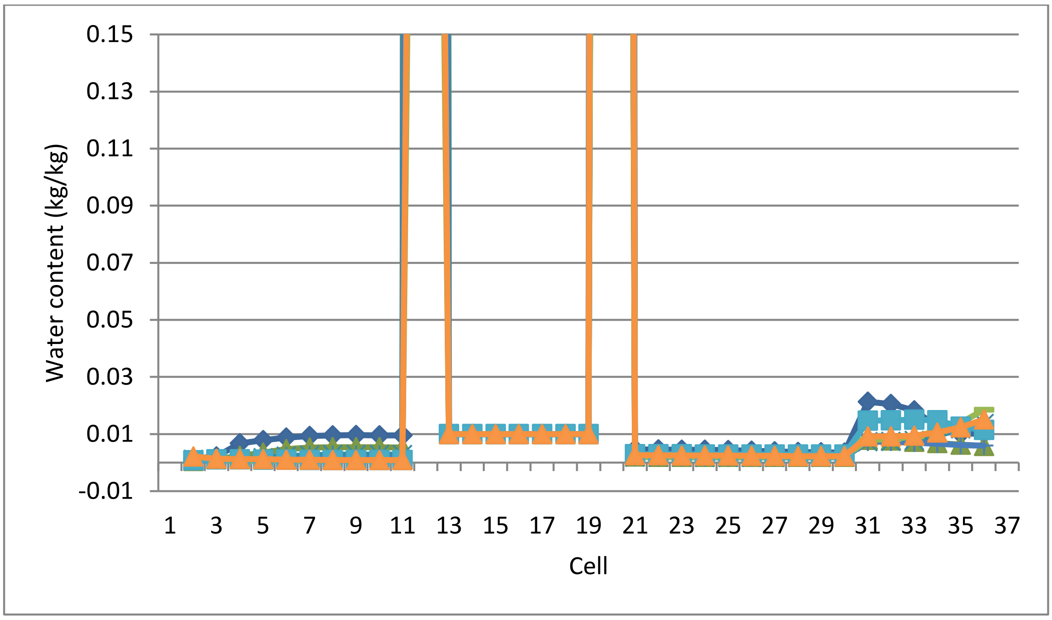

Figure 33. Zoom from the water content profile inside the external wall of the base case.

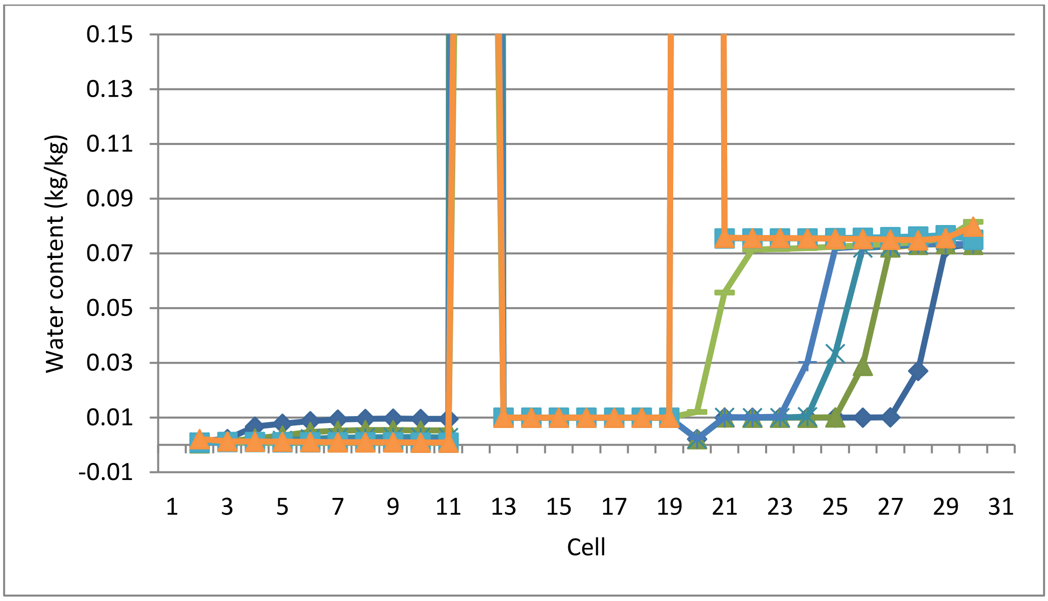

Figure 34. Zoom from the water content profile inside the external wall of the silty clay loam case.

Comparing figures 33 and 34, the difference between the base case and the silty clay loam case is evident when reaching the surface of the non-ventilated chamber with the interior layer (cell 20).The hollow brick partition does not absorb any water and the silty clay loam absorbs more than four times the water absorbed by the plaster layer, being able to see in figure 34 the evolution of water absorption through the year.

5.5 Environmental impact

Having said that rehabilitation would not be justified for the reduction in energy consumption, the environmental impact has been calculated for the scenario of new construction. The impact of the base case includes the impact of the waste treatment of the hollow brick partition and the plaster. In the case of the silty clay loam impact, it has been considered that it is reused without treatment, so the impact caused is the one from the recycling after the life cycle. Table 13 shows the inventory list of the materials used and their corresponding name in the Ecoinvent database.

Table 13. Inventory list of the materials and corresponding name in the Ecoinvent database.

	Component	**Name in the database**	**Amount**
Base case	Electricity	Market for electricity, low voltage (ES) [kWh]	3282.92
	Hollow brick partition	Market for clay brick (GLO) [kg]	9457.54
	Plaster	Market for base plaster (GLO) [kg]	1805.15
Silty clay loam	Electricity	Market for electricity, low voltage (ES) [kWh]	9779.17
	Clay	Market for clay (GLO) [kg]	3499.43
	Sand	Market for sand (GLO) [kg]	999.84
	Silt	Market for sewage sludge, dried (GLO) [kg]	5499.11
Waste treatment	Waste brick	Market for waste brick (GLO) [kg]	3259.73
	Waste plaster	Market for waste mineral plaster (GLO) [kg]	1805.15

Figure 35 shows the environmental impact points of the base case and the silty clay loam case for the event of new construction. It includes the construction, the demolition of the removed materials and energy consumption impact. To be able to appreciate the difference in the electricity and the materials impact, they have been presented separately. The impact of electricity consumption should take into account the consumption during all the life cycle of the building, but for the sake of comparison only the impact points of a year’s consumption are represented. The total environmental impact points for 1, 20 and 50 years are shown in table 14.

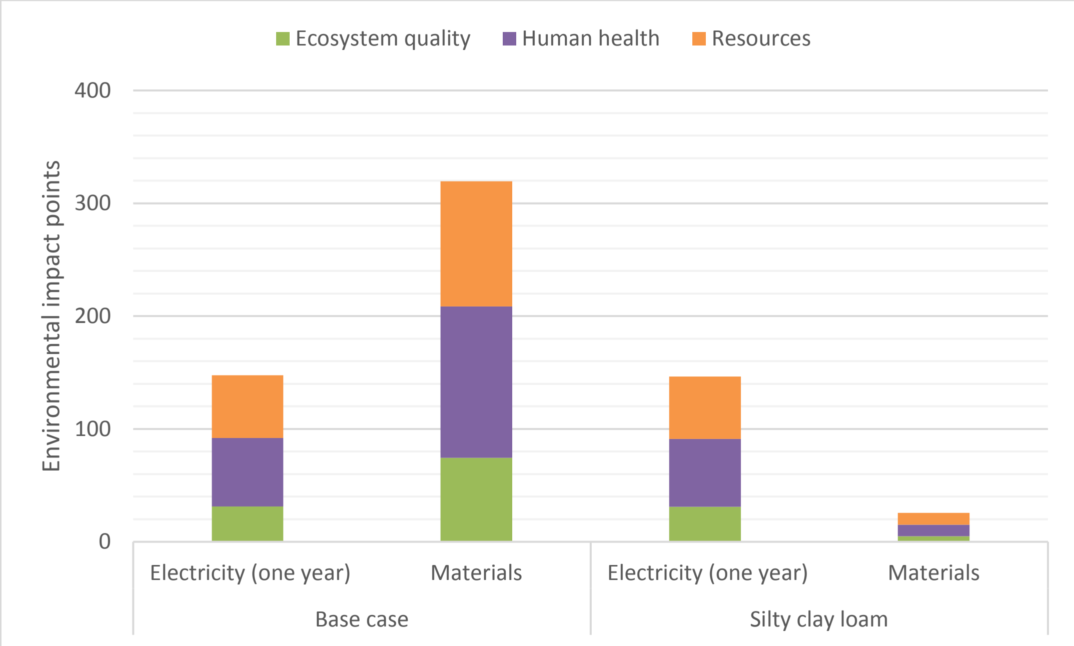

Figure 35. Environmental impact results for the base case and the silty clay loam case for new construction.

Table 14. Total environmental points.

Case	Environmental impact points		
	1 year	20 years	50 years
Base case	467	3271	7697
Silty clay loam	172	2956	7351

As can be observed in the figure, the difference in the electricity impact points between cases is imperceptible. Since the reduction in energy consumption is minimal, the difference in environmental impacts is also very small. Whereas the difference is really appreciable is in the impact of the materials. The silty clay loam has a substantially lower impact than the traditional materials from the base case. The same can be said from the results shown in table 14. The difference observed between both cases is mainly the variation in the materials impacts.

In order to clarify this results and the impacts associated shown in table 13, it is important to analyze the impact of silty clay loam (specifically the silt). This material is usually a waste, and for that reason the impact associated is for its treatment. In the Ecoinvent database, this effect is shown by a negative mass [40] and it must be the user the one to assign the impact properly in his case study. As it has been previously mentioned, in this study it has been supposed that the material is extracted directly from the disposal without previous treatment, having to assume if the material was going to be recycled or not. In this study the worst case scenario has been considered, not obtaining the benefit from the reduction of the impact due to the extraction of the treatment process.

6 Conclusions

The hygrothermal behavior of a single-family detached house in Lleida when substituting the hollow brick partition and plaster layers of the external walls by an earth layer has been studied. Different types of earth have been considered. From the energy consumption results the optimal soil that has been selected for further evaluation, achieving an small reduction in the energy caused by the small difference between the materials. The optimal type of earth has turned out to be the silty clay loam.

The analyzed aspects have been the cost associated to energy consumption, the comfort conditions, the temperature and water content profiles inside the external walls, and the environmental impact derived from the construction, demolitions and energy consumption.

With the silty clay loam layer, energy consumption is reduced by 4%. Proportional to the energy consumption, the gain in the electricity cost with the earth layer is not significant enough to justify the cost of rehabilitation. On the other hand, the difference is notable in the comfort conditions. The earth layer softens temperature changes and reduces the relative humidity inside the house, bringing the comfort conditions closer to the standard.

The water content profiles show that in the base case a significant amount of water was accumulated in the surfaces touching the non-ventilated chamber. This is considerably reduced with the earth layer, given the absorption capacity of the silty clay loam. In some days no water at all is concentrated between its surface and the air chamber.

And last, but not least, when comparing the environmental impact of the earth construction with the conventional materials of the base case the difference is clear. Even though the impact of the energy consumption is almost the same in both cases, the impact of the silty clay loam is twelve times lower than the impact of the materials from the base case.

Given the minimal reduction in energy consumption and cost when implementing the earth layer, using this solution for rehabilitation is discouraged, at least without applying at the same time other measures like change of glazing, implementation of carpentry with thermal bridge breakage and addition of insulation. The effect of this solution applying it along with other measures should be studied further.

Nevertheless, seeing that the earth layer softens the temperature changes and its capacity for water absorption, improving the comfort conditions, it would be encouraged as a possible alternative for new construction.

Additionally, it is recommended to study further the implementation of earth construction for the considerable environmental impact reduction compared to traditional construction materials like clay bricks and plaster.

7 References

[1] IDAE, "Balance del consumo de energía final del año 2015," 2016. [Online]. Available: http://sieeweb.idae.es/consumofinal/bal.asp?txt=Energ%EDa el%E9ctrica&tipbal=f&rep=1. [Accessed: 16-Apr-2017].

[2] S. de Estado de Energía, "Planificación energética indicativa según lo dispuesto en la Ley 2/2011, de 4 de marzo, de Economía Sostenible," 2012.

[3] Ministerio de Indústria,energía y turismo, "La Energía en España 2015." Madrid, 2015.

[4] "Medidas de ahorro de energía y mejora de la eficiencia energética." [Online]. Available: https://ovacen.com/mejora-de-la-eficiencia-energetica/. [Accessed: 14-May-2017].

[5] B. V. Venkatarama Reddy, "Sustainable materials for low carbon buildings," *Int. J. Low-Carbon Technol.*, vol. 4, no. 3, pp. 175–181, Sep. 2009.

[6] S. Dobson, "Rammed earth in the modern world," *Proc. 1st Int. Conf. Rammed Earth Constr. ICREC 2015*, pp. 3–10, 2015.

[7] H. Cagnon, J. E. Aubert, M. Coutand, and C. Magniont, "Hygrothermal properties of earth bricks," *Energy Build.*, vol. 80, pp. 208–217, 2014.

[8] AENOR, "Norma UNE-EN ISO 7730:2006," *http://www.aenor.es/*.

[9] E. Grandjean, "*Wohnphysiologie"*. Zurich, Switzerland, 1972.

[10] J. Beckert, "*Wirkung von Verunreinigungen der Raumluft auf den Menschen*." Düsseldorf, Germany, 1986.

[11] A. M. Papadopoulos and E. Giama, "Environmental performance evaluation of thermal insulation materials and its impact on the building," *Build. Environ.*, vol. 42, no. 5, pp. 2178–2187, May 2007.

[12] Ministerio de Fomento., Colaboradores:, A. (UPC); Cuchí Burgos, A. (Cíclica-U. Pagès, and J. Arcas-Abella, "Estrategia a largo plazo para la rehabilitación energética en el sector de la edificación en España," 2014.

[13] P. Depecker, C. Menezo, J. Virgone, and S. Lepers, "Design of buildings shape and energetic consumption," *Build. Environ.*, vol. 36, no. 5, pp. 627–635, 2001.

[14] H. Sozer, "Improving energy efficiency through the design of the building envelope," *Build. Environ.*, vol. 45, no. 12, pp. 2581–2593, 2010.

[15] S. Domínguez, J. J. Sendra, A. L. León, and P. M. Esquivias, "Towards energy demand reduction in social housing buildings: Envelope system optimization strategies," *Energies*, vol. 5, no. 7, pp. 2263–2287, 2012.

[16] M. Hall and D. Allinson, "Analysis of the hygrothermal functional properties of stabilised rammed earth materials," *Build. Environ.*, vol. 44, no. 9, pp. 1935–1942, 2009.

[17] D. Allinson and M. Hall, "Hygrothermal analysis of a stabilised rammed earth test building in the UK," *Energy Build.*, vol. 42, no. 6, pp. 845–852, 2010.

[18] A. Arrigoni *et al.*, "Reduction of rammed earth's hygroscopic performance under stabilisation: an experimental investigation," *Build. Environ.*, vol. 115, pp. 358–367, Apr. 2017.

[19] L. Soudani *et al.*, "Assessment of the validity of some common assumptions in hygrothermal modeling of earth based materials," *Energy Build.*, vol. 116, pp. 498–511, 2016.

[20] E. Stéphan, A. Caucheteux, S. Tasca-Guernouti, and P. Michel, "Sensitivity analysis of an EnergyPlus simulation model of the ambient humidity in an old building," *13th Conf. Int. Build. Perform. Simul. Assoc.*, pp. 26–28, 2013.

[21] J. Carreras, D. Boer, G. Guillén-Gosálbez, L. F. Cabeza, M. Medrano, and L. Jiménez, "Multi-objective optimization of thermal modelled cubicles considering the total cost and life cycle environmental impact," *Energy Build.*, vol. 88, pp. 335–346, 2015.

[22] F. P. Chantrelle, H. Lahmidi, W. Keilholz, M. El Mankibi, and P. Michel, "Development of a multicriteria tool for optimizing the renovation of buildings," *Appl. Energy*, vol. 88, no. 4, pp. 1386–1394, 2011.

[23] "3D modeling for everyone | SketchUp." [Online]. Available: https://www.sketchup.com/es. [Accessed: 20-Jan-2017].

[24] Código técnico de la Edificación, "Documento básico HE ahorro de energía," 2013.

[25] "OpenStudio | OpenStudio." [Online]. Available: https://www.openstudio.net/. [Accessed: 25-Jan-2017].

[26] "EnergyPlus | EnergyPlus." [Online]. Available: https://energyplus.net/. [Accessed: 26-Jan-2017].

[27] H. M. Künzel, "Simultaneous Heat and Moisture Transport in Building Components. - One- and two-dimensional calculation using simple parameters.," 1995.

[28] EnergyPlus, "Engineering Reference," *US Dep. Energy*, no. c, pp. 1–847, 2010.

[29] "WUFI® 2D | WUFI (en)." [Online]. Available: https://wufi.de/en/software/wufi-2d/. [Accessed: 15-Mar-2017].

[30] "start [- jEPlus.org]." [Online]. Available: http://www.jeplus.org/wiki/doku.php. [Accessed: 18-Apr-2017].

[31] "Main tables - Eurostat." [Online]. Available: http://ec.europa.eu/eurostat/web/energy/data/main-tables. [Accessed: 10-May-2017].

[32] "Ecoinvent." [Online]. Available: https://v32.ecoquery.ecoinvent.org/Home/Index. [Accessed: 24-Apr-2017].

[33] "Apéndice D Zonas climáticas. Documento Básico HE Ahorro de Energía." .

[34] "Lleida, Spain Köppen Climate Classification (Weatherbase)." [Online]. Available: http://www.weatherbase.com/weather/weather-summary.php3?s=591939&cityname=Lleida%2C+Catalu%F1a%2C+Spain&units=. [Accessed: 17-Apr-2017].

[35] Ministerio de Fomento. Gobierno de España, "Catálogo de elementos constructivos del CTE," vol. 3, p. 141, 2010.

[36] A. 55-2010, "ANSI/ASHRAE Standard 55-2010," vol. 2010, p. 42, 2010.

[37] Norma Española, "HS 3 Calidad del aire interior," *Codigo técnico la Edif.*, p. 144, 2009.

[38] M. Kehrer, S. Pallin, A. Harmon, and L. F. Goldberg, *Hygrothermal Simulation of Foundations: Part 1, Soil Material Properties*, no. September. 2012.

[39] "Input Output Reference. Energy Plus Documentation." 2016.

[40] "Methodology of ecoinvent." [Online]. Available: http://www.ecoinvent.org/support/faqs/methodology-of-ecoinvent-3/why-is-the-reference-product-of-the-treatment-activities-negative.html. [Accessed: 20-May-2017].

Annex 1

Tables 15 to 19 show the hygrothermal properties of the materials used in the model.

Table 15. Materials sorption isotherm parameters.

Material	Brick (old)	Clay	Concrete w/c 0.7	Concrete	Interior plaster	Red matt clay brick	Oak old	Air layer
φ^2 1	0	0	0	0	0	0	0	0
W^3 1	0	0	0	0	0	0	0	0
φ 2	0.6	0.01	0.35	0.065	0.5	0.5	0.65	0.5
W 2	1.67	118.2	24	25.5	3.6	1.548	84	1
φ 3	0.8	0.7	0.5	0.113	0.65	0.695	0.8	0.6
W 3	3.34	136.6	30	29.6	5.2	1.742	104	1.5
φ 4	0.93	0.85	0.7	0.329	0.8	0.915	0.93	0.7
W 4	5.01	145.1	45.5	46.1	6.4	2.903	148	2
φ 5	0.96	0.9	0.8	0.582	0.9	1	1	0.8
W 5	6.68	150.5	60	80.1	11	56.115	349	3
φ 6	0.975	0.94	0.9	0.754	0.93	-	-	0.85
W 6	55.11	158.1	85	101	17	-	-	3.4
φ 7	0.985	0.97	0.95	1	0.95	-	-	0.9
W 7	101.87	169.9	106.5	144	19	-	-	5
φ 8	0.99	0.99	0.96	-	0.99	-	-	0.95
W 8	131.93	193.2	114.5	-	113	-	-	7
φ 9	0.99	0.993	0.97	-	0.995	-	-	0.96
W 9	177.02	202.2	124	-	124	-	-	9
φ 10	1	0.996	0.98	-	0.999	-	-	0.97
W 10	195.39	218.1	140	-	328	-	-	11
φ 11	-	0.997	1	-	0.9995	-	-	0.98
W 11	-	227.1	140.1	-	378	-	-	14
φ 12	-	0.998	-	-	1	-	-	0.99
W 12	-	241	-	-	400	-	-	20
φ 13	-	0.9991	-	-	-	-	-	0.995
W 13	-	272.4	-	-	-	-	-	30
φ 14	-	0.9995	-	-	-	-	-	1
W 14	-	299.2	-	-	-	-	-	48
φ 15	-	0.9997	-	-	-	-	-	-
W 15	-	324.8	-	-	-	-	-	-
φ 16	-	0.9999	-	-	-	-	-	-
W 16	-	382.2	-	-	-	-	-	-
φ 17	-	0.99995	-	-	-	-	-	-
W 17	-	413.4	-	-	-	-	-	-
φ 18	-	1	-	-	-	-	-	-
W 18	-	459	-	-	-	-	-	-

[2] Relative humidity fraction (dimensionless)
[3] Moisture content (kg/m^3)

Table 16. Materials suction parameters.

Material	Brick (old)	Clay	Concrete w/c 0.7	Concrete	Interior plaster	Red matt clay brick	Oak old	Air layer
W[4] 1	0	0	0	0	0	0	0	0
D^w [5] 1	0	0	0	0	0	0	0	0
W 2	3.34	112.4	-	101	60	50	104	-
D^w 2	$1.1\cdot10^{-8}$	$1.62\cdot10^{-14}$	-	$3.60\cdot10^{-9}$	$3\cdot10^{-9}$	$1.05\cdot10^{-12}$	$6.3\cdot10^{-13}$	-
W 3	5.01	123.3	-	144	100	70	349	-
D^w 3	$2.8\cdot10^{-8}$	$4.53\cdot10^{-13}$	-	$2.9\cdot10^{-8}$	$1\cdot10^{-7}$	$3.94\cdot10^{-12}$	$8\cdot10^{-11}$	-
W 4	55.11	144.9	-	-	160	90	-	-
D^w 4	$3.56\cdot10^{-7}$	$1.32\cdot10^{-11}$	-	-	$1\cdot10^{-7}$	$1.48\cdot10^{-11}$	-	-
W 5	101.87	195.5	-	-	240	110	-	-
D^w 5	$6.56\cdot10^{-7}$	$7.11\cdot10^{-10}$	-	-	$1.2\cdot10^{-7}$	$5.59\cdot10^{-11}$	-	-
W 6	177.02	296.6	-	-	320	160	-	-
D^w 6	$1.35\cdot10^{-6}$	$3.62\cdot10^{-8}$	-	-	$2.2\cdot10^{-7}$	$1.53\cdot10^{-9}$	-	-
W 7	195.39	357.9	-	-	360	-	-	-
D^w 7	$2.5\cdot10^{-6}$	$1.85\cdot10^{-7}$	-	-	$6\cdot10^{-7}$	-	-	-
W 8	-	441	-	-	380	-	-	-
D^w 8	-	$2.52\cdot10^{-6}$	-	-	$9\cdot10^{-7}$	-	-	-
W 9	-	451.8	-	-	400	-	-	-
D^w 9	-	$5.5\cdot10^{-6}$	-	-	$4.5\cdot10^{-6}$	-	-	-
W 10	-	455.8	-	-	-	-	-	-
D^w 10	-	$9.4\cdot10^{-6}$	-	-	-	-	-	-
W 11	-	457.6	-	-	-	-	-	-
D^w 11	-	$1.48\cdot10^{-5}$	-	-	-	-	-	-
W 12	-	458.3	-	-	-	-	-	-
D^w 12	-	$2.06\cdot10^{-5}$	-	-	-	-	-	-
W 13	-	458.6	-	-	-	-	-	-
D^w 13	-	$2.78\cdot10^{-5}$	-	-	-	-	-	-
W 14	-	458.8	-	-	-	-	-	-
D^w 14	-	$3.40\cdot10^{-5}$	-	-	-	-	-	-
W 15	-	458.9	-	-	-	-	-	-
D^w 15	-	$6.27\cdot10^{-5}$	-	-	-	-	-	-
W 16	-	459	-	-	-	-	-	-
D^w 16	-	$1.21\cdot10^{-4}$	-	-	-	-	-	-

[4] Moisture content (kg/m^3)
[5] Liquid transport coefficient (m^2/s)

Table 17. Materials redistribution parameters.

Material	Brick (old)	Clay	Concrete w/c 0.7	Concrete	Interior plaster	Red matt clay brick	Oak old	Air layer
W[6] 1	0	0	0	0	0	0	0	0
D^w [7] 1	0	0	0	0	0	0	0	0
W 2	3.34	112.4	-	101	60	50	104	-
D^w 2	$1.1 \cdot 10^{-9}$	$9.23 \cdot 10^{-15}$	-	$5 \cdot 10^{-18}$	$3 \cdot 10^{-9}$	$1.05 \cdot 10^{-13}$	$9 \cdot 10^{-13}$	-
W 3	5.01	123.3	-	144	100	70	349	-
D^w 3	$2.8 \cdot 10^{-9}$	$2.59 \cdot 10^{-13}$	-	$5 \cdot 10^{-16}$	$8 \cdot 10^{-9}$	$3.94 \cdot 10^{-13}$	$8 \cdot 10^{-11}$	-
W 4	55.11	144.9	-	-	160	90	-	-
D^w 4	$3.56 \cdot 10^{-8}$	$7.55 \cdot 10^{-12}$	-	-	$8 \cdot 10^{-9}$	$1.48 \cdot 10^{-12}$	-	-
W 5	101.87	195.5	-	-	240	110	-	-
D^w 5	$6.56 \cdot 10^{-8}$	$4.06 \cdot 10^{-10}$	-	-	$1.3 \cdot 10^{-8}$	$5.59 \cdot 10^{-12}$	-	-
W 6	177.02	296.6	-	-	320	160	-	-
D^w 6	$1.35 \cdot 10^{-7}$	$2.07 \cdot 10^{-8}$	-	-	$1 \cdot 10^{-7}$	$1.53 \cdot 10^{-10}$	-	-
W 7	195.39	357.9	-	-	360	-	-	-
D^w 7	$2.5 \cdot 10^{-7}$	$1.05 \cdot 10^{-7}$	-	-	$3 \cdot 10^{-7}$	-	-	-
W 8	-	441	-	-	380	-	-	-
D^w 8	-	$1.44 \cdot 10^{-6}$	-	-	$7 \cdot 10^{-7}$	-	-	-
W 9	-	451.8	-	-	400	-	-	-
D^w 9	-	$3.14 \cdot 10^{-6}$	-	-	$1 \cdot 10^{-6}$	-	-	-
W 10	-	455.8	-	-	-	-	-	-
D^w 10	-	$5.37 \cdot 10^{-6}$	-	-	-	-	-	-
W 11	-	457.6	-	-	-	-	-	-
D^w 11	-	$8.44 \cdot 10^{-6}$	-	-	-	-	-	-
W 12	-	458.3	-	-	-	-	-	-
D^w 12	-	$1.18 \cdot 10^{-5}$	-	-	-	-	-	-
W 13	-	458.6	-	-	-	-	-	-
D^w 13	-	$1.59 \cdot 10^{-5}$	-	-	-	-	-	-
W 14	-	458.8	-	-	-	-	-	-
D^w 14	-	$1.94 \cdot 10^{-5}$	-	-	-	-	-	-
W 15	-	458.9	-	-	-	-	-	-
D^w 15	-	$3.58 \cdot 10^{-5}$	-	-	-	-	-	-
W 16	-	459	-	-	-	-	-	-
D^w 16	-	$6.92 \cdot 10^{-5}$	-	-	-	-	-	-

[6] Moisture content (kg/m^3)
[7] Liquid transport coefficient (m^2/s)

Table 18. Materials diffusion parameters.

Material	Brick (old)	Clay	Concrete w/c 0.7	Concrete	Interior plaster	Red matt clay brick	Oak old	Air layer
φ[8] 1	0	0	0	0	0	0	0	0
μ[9] 1	16	50	147	76	8.3	137.8	223	0
φ 2	0.1	-	0.35	-	-	0.1	-	-
μ 2	15.39	-	147	-	-	137.8	-	-
φ 3	0.9	-	0.5	-	-	0.2	-	-
μ 3	6.68	-	147	-	-	132.5	-	-
φ 4	0.98	-	0.7	-	-	0.3	-	-
μ 4	4.85	-	147	-	-	126.9	-	-
φ 5	-	-	0.7	-	-	0.4	-	-
μ 5	-	-	119	-	-	122.4	-	-
φ 6	-	-	0.8	-	-	0.5	-	-
μ 6	-	-	59.5	-	-	117.6	-	-
φ 7	-	-	0.9	-	-	0.6	-	-
μ 7	-	-	19.2	-	-	113.1	-	-
φ 8	-	-	0.95	-	-	0.7	-	-
μ 8	-	-	4.17	-	-	108.9	-	-
φ 9	-	-	0.96	-	-	0.8	-	-
μ 9	-	-	2.78	-	-	104.6	-	-
φ 10	-	-	0.97	-	-	0.9	-	-
μ 10	-	-	1.25	-	-	100.5	-	-
φ 11	-	-	0.98	-	-	1	-	-
μ 11	-	-	0.625	-	-	96.8	-	-
φ 12	-	-	1	-	-	-	-	-
μ 12	-	-	0.625	-	-	-	-	-

[8] Relative humidity fraction (dimensionless).
[9] Water Vapor Diffusion Resistance factor (dimensionless).

Table 19. Materials moisture content dependent thermal conductivity.

Material	Brick (old)	Clay	Concrete w/c 0.7	Concrete	Interior plaster	Red matt clay brick	Oak old	Air layer
W[10] 1	0	0	0	0	0	0	0	0
k[11] 1	0.4	0.288	1.7	1.373	0.2	0.495	0.152	0.18
W 2	196	98	-	220	650	-	350	-
k 2	0.776	0.28804	-	2.522	1.424	-	0.245	-
W 3	-	134	-	-	-	-	-	-
k 3	-	0.43458	-	-	-	-	-	-
W 4	-	170	-	-	-	-	-	-
k 4	-	0.60896	-	-	-	-	-	-
W 5	-	206	-	-	-	-	-	-
k 5	-	0.80526	-	-	-	-	-	-
W 6	-	242	-	-	-	-	-	-
k 6	-	1.0028	-	-	-	-	-	-
W 7	-	279	-	-	-	-	-	-
k 7	-	1.1799	-	-	-	-	-	-
W 8	-	315	-	-	-	-	-	-
k 8	-	1.3291	-	-	-	-	-	-
W 9	-	351	-	-	-	-	-	-
k 9	-	1.4533	-	-	-	-	-	-
W 10	-	387	-	-	-	-	-	-
k 10	-	1.5579	-	-	-	-	-	-
W 11	-	423	-	-	-	-	-	-
k 11	-	1.6474	-	-	-	-	-	-
W 12	-	459	-	-	-	-	-	-
k 12	-	1.7253	-	-	-	-	-	-

[10] Moisture content (kg/m^3)
[11] Thermal conductivity (W/m·K)

Annex 2

Tables 20 to 24 show the hygrothermal properties of the earths studied. Table 25 shows the thermo-physical properties of the earths studied.

Table 20. Earths sorption isotherm parameters.

Material	Stabilised rammed earth	Clay loam	Silt loam	Silty clay loam
φ 1	0	0	0	0
W 1	0	0	0	0
φ 2	0.3	0.01	0.01	0.01
W 2	24	82.1	65.4	91.4
φ 3	0.4	0.7	0.7	0.7
W 3	25	88	67.2	95.3
φ 4	0.6	0.83	0.8	0.81
W 4	45	90.8	68	97
φ 5	0.8	0.9	0.87	0.89
W 5	55	94	69.1	99.5
φ 6	0.9	0.94	0.92	0.93
W 6	70	97.7	70.7	102.2
φ 7	0.94	0.97	0.95	0.96
W 7	100	104.1	72.9	106.5
φ 8	0.96	0.98	0.97	0.97
W 8	150	108.7	76.2	109.2
φ 9	0.98	0.99	0.98	0.98
W 9	200	118.7	79.7	113.8
φ 10	1	0.993	0.99	0.99
W 10	250	125.1	88.4	124.2
φ 11	-	0.996	0.991	0.991
W 11	-	137.2	90.1	126.1
φ 12	-	0.998	0.994	0.995
W 12	-	156.6	97.8	139.1
φ 13	-	0.999	0.997	0.997
W 13	-	182.3	116.9	154
φ 14	-	0.9992	0.9972	0.9977
W 14	-	192.2	119.3	163.4
φ 15	-	0.9995	0.9981	0.9986
W 15	-	215.9	135.1	184.8
φ 16	-	0.9998	0.9988	0.9991
W 16	-	274.1	159.5	208.8
φ 17	-	0.9999	0.9992	0.9994
W 17	-	325.6	187.2	235.4
φ 18	-	0.99995	0.9993	0.9997
W 18	-	374.2	197.7	291.7
φ 19	-	1	0.9995	0.9998
W 19	-	442	227.3	329.5
φ 20	-	-	1	1
W 20	-	-	439	482

Table 21. Earths suction parameters.

Material	Stabilised rammed earth	Clay loam	Silt loam	Silty clay loam
W 1	25	0	0	0
D^w 1	$1\cdot10^{-9}$	0	0	0
W 2	250	82.6	68.7	93.9
D^w 2	$1\cdot10^{-6}$	$7.97\cdot10^{-15}$	$4.53\cdot10^{-12}$	$2.22\cdot10^{-13}$
W 3	-	86.3	72.5	97.8
D^w 3	-	$1.39\cdot10^{-13}$	$3.64\cdot10^{-11}$	$2.37\cdot10^{-12}$
W 4	-	89.9	80	105.7
D^w 4	-	$6.77\cdot10^{-13}$	$2.93\cdot10^{-10}$	$2.54\cdot10^{-11}$
W 5	-	100.8	91.2	113.5
D^w 5	-	$1.01\cdot10^{-11}$	$1.58\cdot10^{-9}$	$1.02\cdot10^{-10}$
W 6	-	122.6	121.1	152.7
D^w 6	-	$1.52\cdot10^{-10}$	$1.57\cdot10^{-8}$	$2.93\cdot10^{-9}$
W 7	-	158.9	177.2	215.4
D^w 7	-	$1.63\cdot10^{-9}$	$1.32\cdot10^{-7}$	$3.24\cdot10^{-8}$
W 8	-	242.4	308.1	348.7
D^w 8	-	$2.48\cdot10^{-8}$	$1.92\cdot10^{-6}$	$5.24\cdot10^{-7}$
W 9	-	329.5	412.8	454.6
D^w 9	-	$1.94\cdot10^{-7}$	$1.82\cdot10^{-5}$	$5.17\cdot10^{-6}$
W 10	-	420.2	431.5	474.2
D^w 10	-	$2.02\cdot10^{-6}$	$4.97\cdot10^{-5}$	$1.43\cdot10^{-5}$
W 11	-	434.7	436.8	478.5
D^w 11	-	$4.92\cdot10^{-6}$	$1.05\cdot10^{-4}$	$2.38\cdot10^{-5}$
W 12	-	438.7	438.3	480.8
D^w 12	-	$8.2\cdot10^{-6}$	$1.89\cdot10^{-4}$	$4.32\cdot10^{-5}$
W 13	-	440.5	438.7	481.6
D^w 13	-	$1.28\cdot10^{-5}$	$2.95\cdot10^{-4}$	$7.26\cdot10^{-5}$
W 14	-	441.6	438.9	481.7
D^w 14	-	$2.44\cdot10^{-5}$	$5.52\cdot10^{-4}$	$8.50\cdot10^{-5}$
W 15	-	441.7	438.96	481.9
D^w 15	-	$2.55\cdot10^{-5}$	$7.46\cdot10^{-4}$	$1.43\cdot10^{-4}$
W 16	-	441.85	439	481.96
D^w 16	-	$3.54\cdot10^{-5}$	$1.95\cdot10^{-3}$	$1.88\cdot10^{-4}$
W 17	-	441.93	-	482
D^w 17	-	$4.61\cdot10^{-5}$	-	$4.43\cdot10^{-4}$
W 18	-	441.96	-	-
D^w 18	-	$5.93\cdot10^{-5}$	-	-
W 19	-	442	-	-
D^w 19	-	$1.29\cdot10^{-4}$	-	-

Table 22. Earths redistribution parameters.

Material	Stabilized rammed earth	Clay loam	Silt loam	Silty clay loam
W 1	25	0	0	0
D^w 1	$1{\cdot}10^{-9}$	0	0	0
W 2	250	82.6	68.7	93.9
D^w 2	$1{\cdot}10^{-6}$	$4.55{\cdot}10^{-15}$	$2.59{\cdot}10^{-12}$	$1.27{\cdot}10^{-13}$
W 3	-	86.3	72.5	97.8
D^w 3	-	$7.95{\cdot}10^{-14}$	$2.08{\cdot}10^{-11}$	$1.36{\cdot}10^{-12}$
W 4	-	89.9	80	105.7
D^w 4	-	$3.87{\cdot}10^{-13}$	$1.67{\cdot}10^{-10}$	$1.45{\cdot}10^{-11}$
W 5	-	100.8	91.2	113.5
D^w 5	-	$5.8{\cdot}10^{-12}$	$9.01{\cdot}10^{-10}$	$5.82{\cdot}10^{-11}$
W 6	-	122.6	121.1	152.7
D^w 6	-	$8.69{\cdot}10^{-11}$	$8.98{\cdot}10^{-9}$	$1.67{\cdot}10^{-9}$
W 7	-	158.9	177.2	215.4
D^w 7	-	$9.31{\cdot}10^{-10}$	$7.53{\cdot}10^{-8}$	$1.85{\cdot}10^{-8}$
W 8	-	242.4	308.1	348.7
D^w 8	-	$1.62{\cdot}10^{-8}$	$1.1{\cdot}10^{-6}$	$3{\cdot}10^{-7}$
W 9	-	329.5	412.8	454.6
D^w 9	-	$1.11{\cdot}10^{-7}$	$1.04{\cdot}10^{-5}$	$2.95{\cdot}10^{-6}$
W 10	-	420.2	431.5	474.2
D^w 10	-	$1.15{\cdot}10^{-6}$	$2.84{\cdot}10^{-5}$	$8.18{\cdot}10^{-6}$
W 11	-	434.7	436.8	478.5
D^w 11	-	$2.81{\cdot}10^{-6}$	$6.01{\cdot}10^{-5}$	$1.36{\cdot}10^{-5}$
W 12	-	438.7	438.3	480.8
D^w 12	-	$4.69{\cdot}10^{-6}$	$1.08{\cdot}10^{-4}$	$2.47{\cdot}10^{-5}$
W 13	-	440.5	438.7	481.6
D^w 13	-	$7.31{\cdot}10^{-6}$	$1.68{\cdot}10^{-4}$	$4.15{\cdot}10^{-5}$
W 14	-	441.6	438.9	481.7
D^w 14	-	$1.39{\cdot}10^{-5}$	$3.16{\cdot}10^{-4}$	$4.86{\cdot}10^{-5}$
W 15	-	441.7	438.96	481.9
D^w 15	-	$1.46{\cdot}10^{-5}$	$4.26{\cdot}10^{-4}$	$8.17{\cdot}10^{-5}$
W 16	-	441.85	439	481.96
D^w 16	-	$2.02{\cdot}10^{-5}$	$1.12{\cdot}10^{-3}$	$1.07{\cdot}10^{-4}$
W 17	-	441.93	-	482
D^w 17	-	$2.63{\cdot}10^{-5}$	-	$2.53{\cdot}10^{--4}$
W 18	-	441.96	-	-
D^w 18	-	$3.39{\cdot}10^{-5}$	-	-
W 19	-	442	-	-
D^w 19	-	$7.37{\cdot}10^{-5}$	-	-

Table 23. Earths diffusion parameters.

Material	Stabilised rammed earth	Clay loam	Silt loam	Silty clay loam
φ 1	0.32	0	0	0
μ 1	7.7	50	50	50
φ 2	0.43	-	-	-
μ 2	8	-	-	-
φ 3	0.58	-	-	-
μ 3	9	-	-	-
φ 4	0.75	-	-	-
μ 4	10.2	-	-	-
φ 5	0.8	-	-	-
μ 5	11.2	-	-	-
φ 6	0.95	-	-	-
μ 6	14.5	-	-	-

Table 24. Earths moisture content dependent thermal conductivity.

Material	Stabilised rammed earth	Clay loam	Silt loam	Silty clay loam
W 1	0	0	0	0
k 1	0.85	0.35	0.369	0.318
W 2	0.6	79	65	90
k 2	1.158	0.35	0.369	0.318
W 3	-	115	102	129
k 3	-	0.514	0.497	0.426
W 4	-	152	140	168
k 4	-	0.733	0.671	0.554
W 5	-	188	177	208
k 5	-	0.938	0.851	0.725
W 6	-	224	215	247
k 6	-	1.131	1.048	0.925
W 7	-	261	252	286
k 7	-	1.304	1.236	1.119
W 8	-	297	289	325
k 8	-	1.445	1.386	1.278
W 9	-	333	327	364
k 9	-	1.558	1.502	1.404
W 10	-	369	364	404
k 10	-	1.651	1.593	1.504
W 11	-	406	402	443
k 11	-	1.729	1.667	1.588
W 12	-	442	439	482
k 12	-	1.797	1.73	1.66

Table 25. Thermo-physical properties of the earths studied.

Material	**Stabilized rammed earth**	**Clay loam**	**Silt loam**	**Silty clay loam**
k (W/m·K)	0.643	0.35	0.369	0.318
ρ (kg/m^3)	1900	1361	1439	1284
Cp (J/kg·K)	868	850	850	850
Porosity (m^3/m^3)	0.295	0.476	0.448	0.504